UNIVERSITÉ DE MONTRÉAL

DESIGN OF AN UNDERACTUATED COMPLIANT GRIPPER FOR
SURGERY USING NITINOL

MARIO ARTURO DORIA DI COSTANZO
DÉPARTEMENT DE GÉNIE MÉCANIQUE
ÉCOLE POLYTECHNIQUE DE MONTRÉAL

Canada

UNIVERSITÉ DE MONTRÉAL

ÉCOLE POLYTECHNIQUE DE MONTRÉAL

Ce mémoire intitulé :

DESIGN OF AN UNDERACTUATED COMPLIANT GRIPPER FOR
SURGERY USING NITINOL

présenté par : DORIA DI COSTANZO Mario Arturo

en vue de l'obtention du diplôme de : Maîtrise ès sciences appliquées

a été dûment accepté par le jury d'examen constitué de :

M. DE SANTIS Romano, Ph.D., président

M. BIRGLEN Lionel, Ph.D., membre et directeur de recherche

M. AUBIN Carl-Éric, Ph.D., membre

To my wife, my brother, my parents.

ACKNOWLEDGMENTS

I am grateful to my supervisor for his support, help, and encouragement. Dr. Lionel Birglen was always eager to discuss my work and suggest improvements. He was very kind and patient and I have a lot of respect for him as a teacher and as a person.

My time in the École Polytecnique de Montréal has been made memorable by the teachers I met and the friends I made. Very warm thanks to my friends that made this experience all the better. In particular I would like to thank Silvio and Claudia in Montreal, and to all my great friends from back home.

My family has always been very close to me, and even though they live back in Mexico, they have been a great source of support. I deeply thank my wife, my brother, and especially my parents for their support without which this thesis would never have happened.

RÉSUMÉ

Dans ce mémoire, le développement d'un préhenseur sous actionné compliant est présenté. Un préhenseur sous actionné qui peut s'adapter à l'objet saisi devrait mettre en valeur la productivité et les capacités de l'utilisateur dans le domaine chirurgical. Le problème principal était de développer un préhenseur à cinq phalanges avec un performance acceptable étant donné les restrictions imposées par le sous actionnement. Il peut être utilisé comme extrémité d'un instrument endoscopique ou comme outil d'un robot. Une nouvelle architecture est présentée dans ce mémoire et optimisée en utilisant comme critères des résultats récents de ce domaine de recherche. Des procédures d'optimisation évoluées ont été nécessaires pour obtenir la géométrie du mécanisme de transmission car il s'agit d'un préhenseur sous actionné et donc très complexe. Un deuxième objectif était de développer un mécanisme supplémentaire incorporé pour distribuer le mouvement d'actionnement aux deux doigts du préhenseur. En effet, la distribution de mouvement est critique lorsque le préhenseur tente de saisir des objets asymétriques. Finalement, des simulations numériques du préhenseur résultant avec des matériaux différents et une analyse de la sensibilité du préhenseur sont présentées et discutées. En conclusion, des simulations numériques préliminaires à des validations expérimentales indiquent que le préhenseur possède les performances attendues.

ABSTRACT

An end-effector for robots or a surgical tool that can adapt itself to the grasped object would enhance the productivity and capabilities of the user. In this thesis, the development of an underactuated compliant gripper is presented. It can be used as the end-effector of an endoscopic instrument or a robot. It is a novel design optimized using as criteria recent theoretical advances presented in the field. Optimization procedures are required to obtain the geometry of the transmission mechanism because of its underactuated nature. A driving mechanism further incorporated to distribute actuation to both fingers of the gripper while aiming at managing the grasping of asymmetrical objects without requiring supplementary inputs is also discussed. Finally, the results of numerical simulations of the gripper with different materials are presented and discussed.

CONDENSÉ EN FRANÇAIS

Ce mémoire décrit le développement d'un préhenseur compliant sous actionné destiné à être utilisé en chirurgie. Il est basé sur un article soumis au journal de dispositifs médicaux de la ASME. La chirurgie est un champ médical qui a été révolutionné par le développement des techniques chirurgicales minimalement invasives. La laparoscopie est une de ces techniques devenue très populaire car elle réduit la mortalité et la douleur postopératoire. Avec des instruments fins introduits dans l'abdomen, le chirurgien peut réaliser fidèlement les gestes de la chirurgie traditionnelle.

Parmi les instruments utilisés, on trouve les pinces pour prendre et manipuler les organes et tissus dans le corps humain. Ces pinces ne s'adaptent pas aux objets et elles peuvent être améliorées. Le préhenseur décrit dans ce travail s'adapte de façon mécanique à l'objet pris et distribue la force appliquée sur l'objet sans électronique ni capteurs. De cette façon, l'objet manipulé est moins traumatisé qu'avec l'approche traditionnelle.

Le préhenseur présenté est fait avec du Nitinol. Le Nitinol est un alliage biocompatible de nickel titane presque équiatomique. Il est intéressant pour ses propriétés mécaniques particulières, principalement l'effet de mémoire de forme et la super élasticité. Cette dernière propriété nous permet de faire des articulations compliantes à grand débattement.

Le sous actionnement est un concept assez vieux dans la robotique, il s'agit d'une propriété des mécanismes qui leur permet d'avoir moins d'actionneurs que de degrés de liberté. Cette propriété est accordée au préhenseur grâce aux mécanismes différentiels qui transforment un mouvement d'actionnement en plusieurs sorties de force. Le sous actionnement permet au préhenseur de s'adapter à l'objet pris sans nécessiter une architecture de contrôle complexe. Le préhenseur s'adapte mécaniquement à l'objet sans qu'il y ait de contrôle externe et avec un seul actionneur.

Pour cette raison, le processus d'optimisation doit tenir compte des conséquences liées aux choix des paramètres du préhenseur.

Le préhenseur est composé de deux doigts robotiques, un mécanisme de transmission qui distribue le couple d'actionnement aux différentes phalanges du doigt, un mécanisme de base qui convertit une force d'actionnement en deux couples pour les mécanismes de transmission.

La conception du préhenseur a été faite en cinq phases qui sont :

1. Conception des articulations.

2. Conception du doigt.

3. Optimisation du mécanisme de transmission.

4. Optimisation du mécanisme de base.

5. Simulation numérique.

Conception des Articulations

On désire que les articulations du préhenseur soient flexibles et que tout le préhenseur puisse être usiné à partir d'une même plaque de Nitinol. C'est pour cette raison que les articulations en charnière et avec des coins arrondis ont été choisies. Deux types d'articulations ont été réalisées : le premier type est asymétrique avec une forme telle que l'objet pris par le préhenseur ne peut bloquer son mouvement ; le second type concerne les articulations dans le mécanisme de transmission et a été pensé de manière à maximiser la vie du préhenseur.

Les conclusions de travaux antérieurs sur le développement des préhenseurs sous actionnés ont montré des difficultés avec les articulations. En effet, le processus d'usinage requiert une épaisseur assez large des articulations, notamment celle de la tige centrale. La force d'actionnement devient très grande et cela devient donc nécessaire d'actionner le préhenseur avec un actuateur électrique.

Des simulations numériques ont été faites et une analyse de fatigue nous donne comme résultat une vie des articulations très longue. Il est possible d'élargir la vie des articulations grâce à une tige centrale plus mince. Cette action aurait cependant un effet nocif sur le reste de la performance car le préhenseur deviendrait très fragile.

Conception du Doigt

Les doigts sous-actionnés peuvent être étudiés comme l'ensemble de plusieurs mécanismes. Le doigt robotique et les mécanismes de transmission associés ont comme résultat la capacité d'auto-adaptation du préhenseur. Les doigts du préhenseur ont chacun cinq phalanges et la longueur totale a été choisie pour être semblable aux pinces laparascopiques usuelles. Chaque doigt du préhenseur a donc cinq degrés de liberté. Le mécanisme de transmission distribue le couple d'entrée à toutes les articulations du doigt. Un mécanisme de base additionnel convertit une force (car c'est la méthode d'actionnement habituelle en laparoscopie) en deux couples, un pour chaque doigt du préhenseur.

Plusieurs types de mécanismes de transmission ont été étudiés. On a finalement retenu trois types de mécanismes montrant des bons résultats pour être étudiés en détail. La première analyse cherchait à écarter les mécanismes qui ne pourraient jamais finir la séquence de fermeture à cause des collisions entre leur membrures internes. L'architecture une, (cf. 3.5(a)) est le mécanisme le plus simple pour un doigt robotique à cinq phalanges. On peut l'étudier aussi comme un doigt à deux phalanges avec la phalange proximale divisée en quatre. C'est une idée intéressante parce que ce nouveau doigt pourrait offrir une meilleure distribution des forces sur l'objet pris en ayant cinq forces de contact au lieu de deux.

Pour choisir le meilleur mécanisme, un processus d'optimisation a été réalisé pour chacune de ces architectures. L'optimisation est basée sur l'analyse des forces de contact du doigt sur l'objet saisi. Ci-dessous sont décrits les critères de l'optimisation

et leurs résultats.

Optimisation du mécanisme de transmission

Chaque mécanisme de transmission est défini par ses paramètres géométriques. L'optimisation de ces paramètres a été faite à l'aide d'un algorithme génétique. La fonction objective est la note donnée à chaque ensemble de paramètres en fonction des critères décrits ci-dessous :

1. Les forces de contact doivent toutes être positives.

2. Le couple qui agit sur la dernière phalange du doigt doit être positif.

3. La projection sur la dernière phalange de l'intersection entre les deux lignes associées aux membrures attachées à cette phalange doit être à l'intérieur de celle-ci.

Des objets typiques à saisir ont été développés afin de voir la performance du doigt dans des cas pratiques. Pendant ces prises, la force résultante qui agit sur l'objet doit pousser l'objet vers la paume du préhenseur.

Quand le processus d'optimisation utilise des objets typiques, le but est d'évaluer la performance du doigt robotique pendant la prise d'objets circulaires petits et grands. Il est important de mentionner que pendant les prises de petits et grands objets circulaires, le doigt n'utilise que deux phalanges pour les prendre. Pour profiter de la symétrie, on considère que le reste des phalanges se touchent entre elles, comme si les doigts pinçaient un cheveux. Les résultats sont très intéressants, mais il faudrait continuer à développer le modèle mathématique. Dans ce cas-là, on considère qu'il y a seulement une force de contact entre les phalanges et cette force-là est située au milieu de la phalange. C'est un modèle simplifié qui ne considère pas le cas où le doigt pourrait arriver à avoir cette configuration. Sans un modèle théorique qui décrive le chemin pris par le doigt robotique et ne pouvant pas faire

une simulation numérique (simulation des éléments finis) car celle-ci prend trop de temps, la possibilité de prédire la configuration finale du doigt en saisissant un objet très petit n'est pas faisable. Un modèle théorique de ce cas-là requiert des équations très détaillées du mécanisme et particulièrement des articulations compliantes. De plus, si on prend en compte la super élasticité du Nitinol dans le modèle, l'analyse devient onéreuse et on perd les avantages offerts par le modèle disponible

Les architectures qui rempliront toutes ces conditions seront ensuite notées en fonction des critères suivant :

1. La déformation dans chaque articulation du mécanisme de transmission est comparée avec la valeur maximale permise, les cas avec une déformation minimale recevront une note supérieure.

2. Les forces de contact sont additionnées et divisées par la force d'entrée dans le mécanisme de transmission, ce critère favorise les architectures qui reflètent fidèlement l'effort d'actionnement à la force totale exercée sur l'objet.

3. La déviation standard des forces de contact est évaluée car elle caractérise l'uniformité de la saisie, le but étant de favoriser les architectures qui génèrent des forces égales à chaque phalange.

Finalement, ces critères sont multipliés entre eux et le résultat est la note finale donnée à l'architecture évaluée.

Les résultats de l'optimisation sont intéressants et donnent un mécanisme de transmission pour les doigts du préhenseur. Il faut noter que la fonction objective du processus d'optimisation est très sensible aux variations des paramètres géométriques. Pour cette raison, une analyse de sensibilité a été faite en utilisant l'analyse de variance (ANOVA) qui permet d'identifier des ensembles critiques de paramètres.

Optimisation du mécanisme de base

Le mécanisme qui transforme une force en deux couples pour les mécanismes de transmission a été optimisé séparément. Le but de l'optimisation est que dans un mouvement de fermeture, si un doigt est bloqué, le mécanisme transmette un couple plus grand à celui-ci sans s'arrêter. Ce mécanisme émule le mouvement fait par un actuateur linéaire utilisé dans une chirurgie laparoscopique.

L'optimisation a été faite avec un algorithme génétique, comme cela a été fait pour l'optimisation du doigt robotique. Un index qui caractérise la performance de chaque mécanisme de base a été fait en regardant si :

1. Quand les deux angles ($\theta_{A1,A2}$) sont égaux, leurs couples d'actionnement transmis aux doigts robotiques doivent avoir une magnitude égal.

2. Quand les deux angles sont différents, la membrure avec l'angle le plus petit doit transmettre le couple avec la magnitude la plus grande.

3. La performance du mécanisme est symétrique, cela veut dire que si on échange les angles, on aura le même résultat.

La figure 3.12 présente le résultat de l'optimisation du mécanisme de base. Le résultat est satisfaisant et avec le mécanisme de transmission, on obtient le schéma final du préhenseur. La figure 1 montre un prototype du préhenseur fait en aluminium.

Discussion des Résultats

Le préhenseur à été optimisé en regardant en premier les aspects mécaniques de sa performance. L'intention du travail était de tester la théorie disponible pour vérifier les conclusions sur la performance d'un manipulateur sous actionné quand il est optimisé avec un critère basé sur les forces de contact. Même si le préhenseur est pensé pour son utilisation dans une chirurgie, le processus d'optimisation contenait

Figure 1 Prototype du préhenseur fait en aluminium.

peu des critères liés à la chirurgie laparoscopique. La taille des doigts robotiques a été limitée pour ressembler à la taille des manipulateurs commerciaux et le processus d'optimisation pénalisait les candidats qui étaient trop encombrants. Il pourra certes être difficile d'insérer le préhenseur dans le corps humain, mais grâce à la super élasticité du Nitinol, il est possible de comprimer le manipulateur et de le déployer dans le corps humain où il reprendrait sa forme habituelle. C'est un domaine de recherche très actif et des travaux de recherche ultérieurs pourraient se centrer sur la miniaturisation du préhenseur. Une possibilité est de réduire le nombre de phalanges en utilisant le processus d'optimisation présenté dans ce travail.

En ce qui concerne le nombre de phalanges des doigts robotiques, on peut avoir une meilleure distribution de forces de contact en ayant un nombre plus grand de phalanges. Il faut cependant remarquer qu'avec un nombre plus grand de phalanges, la condition d'avoir toujours des forces positives de contact devient une limitation très restrictive pour le processus d'optimisation. Par exemple, l'architecture une (cf. Figure 3.5(a)) développe très facilement des forces de contact nulles ou

négatives. L'architecture deux (cf. Figure 3.5(b)), avec un soutien sur la première, troisième et cinquième phalanges, développe en revanche moins de forces de contact négatives. C'est ce support donné par le mécanisme de transmission au doigt robotique qui permet à cette architecture-ci d'avoir les meilleurs résultats. Même si les phalanges deux et quatre ont parfois des forces de contact négatives et si on adopte un critère moins strict qui ne considère pas comme crucial une force de contact négative sur ces phalanges, la performance du doigt robotique sera satisfaisante. Ainsi, les deux phalanges peuvent être considérées comme des extensions de longueur qui permettent au doigt robotique d'offrir une meilleure prise qu'un doigt à trois phalanges avec une membrure entre chaque phalange et le mécanisme de transmission. Autrement dit, l'architecture deux est plus flexible parce qu'elle demande une flexion plus petite aux articulations du doigt grâce à ses cinq phalanges. Cependant, il est important de souligner qu'en raison de ses cinq phalanges, elle développe des forces de contact négatives.

Comme cela est décrit dans [Laliberté and Gosselin, 2001], la condition qui stipule que la longueur de toutes les membrures C_i doit être la plus petite possible est validée dans le processus d'optimisation fait ici. Les résultats de l'algorithme d'optimisation génétique montrent que les longueurs des membrures C_i sont toujours proches de leurs limites minimales.

L'analyse de sensibilité est un nouveau développement qui, à la connaissance de l'auteur, n'a jamais été fait avec un doigt sous actionné. Une expérience factorielle à deux niveaux suivie par une analyse de la variance (ANOVA) de résultats nous présente l'évidence statistique d'un changement de la performance du doigt. Cette analyse met en valeur la sensibilité de la fonction objective aux petits changements des paramètres géométriques constitutifs du doigt. Au début, l'analyse avait été envisagée comme une mesure de sensibilité ; en augmentant peu à peu les niveaux haut et bas de l'expérience et en les analysant, on peut montrer l'évidence statistique que la performance du préhenseur changera. Dans le cas du préhenseur présenté ici,

même le processus d'usinage (EDM) aurait un effet sur sa performance. Cela est une conséquence de la condition obligeant à toujours avoir des forces de contacts positives.

Étant donné que faire des tests avec un prototype du préhenseur serait très onéreux, il a donc fallu se contenter de simulations par éléments finis. Le logiciel commercial *ANSYS* a été employé en raison de son module qui simule le comportement des alliages à mémoire de forme. Cela permet de donner des résultats très précis même si le matériau ne se comporte pas linéairement. Les données sur le Nitinol ont été trouvées dans la littérature, plus particulièrement les données sur son comportement en fatigue. Du fait qu'on envisage l'éventuelle utilisation du préhenseur dans une chirurgie laparoscopique, la caractérisation du Nitinol a été faite de façon à exploiter sa super élasticité plutôt que sa mémoire de forme. Si un préhenseur est utilisé, il devrait être utilisé au-dessus de sa température finale d'austénite, dans ce cas précis, au-dessus de 29°C. La base du mécanisme a été actionnée avec un déplacement linéaire afin d'avoir un bon résultat dans la simulation par éléments finis et afin d'aider à la convergence. Cela a été fait au lieu d'appliquer une force sur la base du préhenseur afin de l'actionner.

Conclusion

La simulation numérique par éléments finis du préhenseur résultant montre une bonne performance du préhenseur pour la saisie d'objets différents, même dans les situations où l'objet pris n'est pas symétrique. La force nécessaire pour actionner le préhenseur est élevée à cause de l'épaisseur et de la longueur des articulations. En conséquence, il est nécessaire d'utiliser un actuateur électrique pour bouger le préhenseur. L'épaisseur minimale des articulations est une condition donnée par le processus d'usinage du préhenseur. Dans un travail futur, la réduction de l'épaisseur des articulations aura comme résultat de faciliter l'actionnement du préhenseur.

xvii

La fonction objective utilisée dans le processus d'optimisation est très sensible aux changements des paramètres. On peut apprécier ses effets plus particulièrement dans le processus d'optimisation dans les résultats de l'analyse de sensibilité. Cela est dû au critère des forces de contact et à la condition qui implique que toutes les forces soient positives. Il faut souligner que, bien que cette condition soit très importante dans la théorie, on peut relâcher la condition dans la réalité. Des forces de contact négatives peuvent bien sûr donner comme résultat un préhenseur qui n'arrive pas à prendre un objet. Cependant, si on fait une analyse cas par cas des forces de contact et si, dans le cas du projet présenté ici, on étudie seulement les forces de contact sur les phalanges une, trois et cinq, la performance du préhenseur ne sera pas inférieure. Dans le cadre d'une recherche future, on pourrait étudier les forces de contact sur la phalange distale et s'intéresser aux analyses éventuelles sur sa stabilité en prenant en compte de nouveaux critères.

La sensibilité de la fonction objective du processus d'optimisation est due au fait que le critère requérant que toutes les forces de contact soient positives est très strict. La simulation numérique montre que le critère pourrait être relâché mais cela nécessiterait des développements sur l'analyse des forces de contact.

L'utilisation de l'analyse de la variance (ANOVA) a montré son utilité pour déterminer la viabilité d'un préhenseur. Malgré le fait que l'analyse a montré plusieurs interactions statistiquement significatives, le résultat est très intéressant. En effet, plus le nombre de phalanges augmente, plus la sensibilité du doigt robotique augmente. Ceci dit, la condition qui implique que les forces de contact soient positives est valide et fonctionne très bien pour concevoir des doigts robotiques avec peu de phalanges. Plus il y a de phalanges, plus l'espace de travail est limité et plus il est difficile de trouver un candidat qui remplit toutes les conditions du processus d'optimisation. Un travail futur pourra reprendre l'analyse des forces de contact et développer des conditions où il ne sera pas nécessaire d'avoir toutes les forces de contact positives dans tous les cas d'utilisation du préhenseur.

TABLE OF CONTENTS

LIST OF APPENDICES

LIST OF FIGURES

LIST OF NOTATIONS AND SYMBOLS

ANOVA   Analysis of Variance

DOF: Degree Of Freedom

EDM: Electrical Discharge Machining

FEA: Finite Element Analysis

FEM: Finite Element Method

GA: Genetic Algorithm

MIS: Minimally Invasive Surgery

NiTi: Nitinol

SMA: Shape Memory Alloy

LIST OF TABLES

INTRODUCTION

The idea of making a machine do our menial, complex, or dangerous tasks is very attractive. The search for efficiency in our industrial endeavors requires doing more with less. Robots, as we commonly see them today, are part of the effort driving to fulfill these worthy goals. We build them stronger and able to withstand operating in ever-harsher environments where humans cannot. For them to take the place of a human, they require to have a baseline, a basic set of capabilities allowing them to successfully carry out the tasks put out for them. Part of those tasks are the grasping and manipulation of objects. A human hand is an excellent tool both for manipulation and grasping, having many muscles, joints and nerves [Schmidt and Ulrich, 2004]. For robots to successfully mimic a human hand, they need appropriate end-effectors. Numerous research initiatives have been conducted in the past to create adequate robotic end-effectors that can match the human hand in terms of performance and versatility. In a way, the adaptability of the human hand can be thought of as the ultimate goal of robotic end-effectors [Birglen et al., 2008]. Several research labs have embarked on developing such *robotic hands* and many interesting prototypes have resulted. The designs put forward usually require a complex control architecture, making them expensive and sometimes may lead to poor grasping performance due to a demanding control [Birglen et al., 2008]. In fact, although a gripper is generally unable to manipulate an object, it can grasp it very well. This approach, with robotic grippers that do not try to mimic hand but instead focus on only one task, is the one more usually followed with industrial robots. Each end-effector is however designed in general for one task only. Underactuation opens the door to mechanism self-adaptability, bringing together the advantages of single-task grippers with the versatility offered by robotic hands. To prove the worthiness of the concept, one of the SARAH Hands from [Laliberté and Gosselin, 2003] which

is underactuated, is expected to be used in outer space next year.

Underactuation is a relatively old concept in robotics, it expresses the property of a robotic system to have less actuators than degrees of freedom. The basic premise is to use a relatively simple gripper that will adapt itself to the object being grasped. This capability is afforded to the device by the use of differential mechanisms that distribute one input into several outputs. A gripper taking advantage of underactuation is beneficial for a robotic system as a whole since it simplifies the required control architecture.

Surgery is one field that has been revolutionized by the use of minimally invasive techniques (MIS). Operations are conducted through small incisions into the body by using flexible instruments with appropriate end-effectors. This is another area where an underactuated gripper can perform very well. It can aid a surgeon by allowing a more effective grasp by exploiting the shape-adaptation capabilities afforded by underactuation. Figure 1 illustrates a rigid gripper in a laparoscopic surgery. An end-effector adapting itself to the grasped organ or tissue can reduce the damage done on biological material by deforming it the least in order to securely grasp it.

The objective of this research is to develop an underactuated gripper able to be eventually used in MIS. The focus of this research is in the mechanical aspects while envisioning its use in surgery. This gripper is to have two fingers and resemble a common laparoscopic pincer. Underactuated grippers do not require a dedicated control architecture and can provide a cheaper alternative to more complicated end-effectors without losing functionality, making it attractive for surgical use. To avoid an unnecessarily complicated sterilization procedure the gripper is made out of Nitinol. Furthermore, this material offers other important advantages useful in a compliant gripper. Nitinol is a shape memory alloy (SMA) that exhibits super
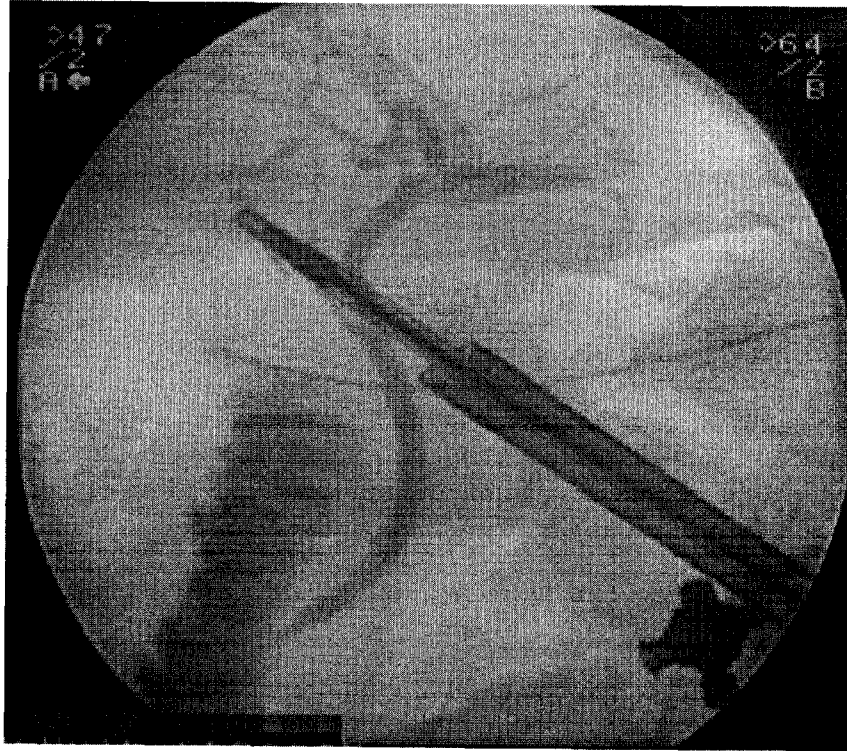
Figure 1 X-Ray of a conventional laparoscopic grasper during surgery [Wikimedia, 2008].

elastic properties. By taking advantage of super elasticity and compliant joints, the size of the gripper can be reduced and underactuation is achieved without requiring extra elements like springs.

Some of the tools available for surgeons in endoscopic surgeries are holders, scalpels, needle holders, scissors, and graspers. Graspers are usually made of strong materials, for example surgical-grade stainless steel. This material offers the advantage of being easy to sterilize, but it is not suitable for building compliant joints due to the force required to flex them. Usually, end-effectors are attached to laparoscopic tools and together they attain sizes up to 60 cm. The end-effectors alone have sizes that go from one to almost four centimeters, and are used in different types of situations such pulling or holding objects in place. The jaw usually opens up to 30° and in some cases up to 60°. These grippers are used to hold soft tissue or

hard objects (e.g., bones) as they function as common pincers. There are various types of laparoscopic tools on the market, some of them focus on the force feedback afforded to the surgeon, others offer a larger number of degrees of freedom (up to seven), while finally other types are meant for robot-assisted surgeries and therefore are conceived to perform more precise movements. The end-effector presented in this work could afford the surgeon haptic capabilities as well as a more dextrous grip on objects by virtue of its underactuated shape-adapting nature. The
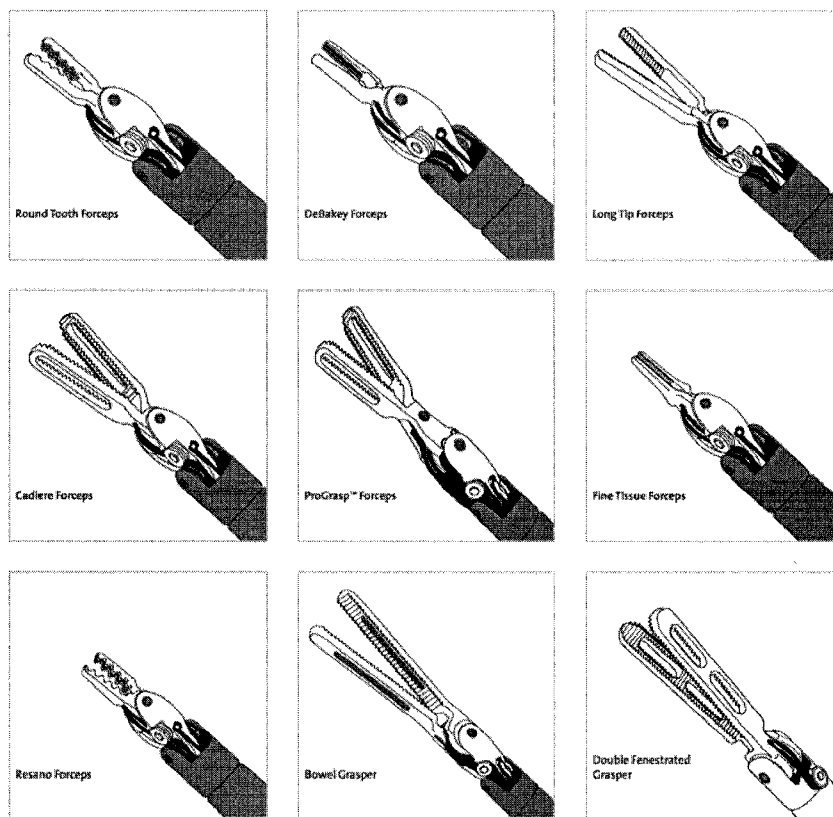
Figure 2 Some common endoscopic instruments [Intuitive Surgical, 2008a].

gripper presented in this thesis is the result of a series of optimization procedures that take into account various different performance criteria. The mechanical aspects took precedence in the criteria used in the various optimization procedures carried out. However, constraints due to the intended surgical usage of the gripper

such as biocompatibility, temperature, and size were taken into account before the optimization of mechanical properties. The development of the gripper is divided into three stages. First, the conception of the finger and its joints, considering the constraints imposed by the use of Nitinol. Second, the transmission mechanism which distributes an actuating torque to all the phalanges of the finger. Third, the driving mechanism that converts an input force into actuating torques for the fingers. Finally, a finite element analysis (FEA) is done on the resulting design and its results are presented.

Thesis Organization

The whole thesis is based on a submitted article to the ASME Journal of Medical Devices and has six chapters: three chapters framed by an introduction and a conclusion. The first chapter covers the existing literature related to underactuated robotic hands. Chapter 2 presents the work outline and how the article fits with the research objectives. Chapter 3 presents the submitted article. Finally, Chapter 4 presents a discussion of the results obtained in this thesis.

CHAPTER 1

LITERATURE REVIEW

The attempt to mimic the human hand with a robotic one is fraught with perils. The human hand has approximately 20 degrees of freedom, twice the number of muscles and thousands of nerve endings [Schmidt and Ulrich, 2004]. It is no wonder that to emulate it, a robotic hand requires a complex control architecture. To succeed with this endeavor, particular emphasis has been placed on the reduction of the number of degrees of freedom, thereby reducing the required number of actuators. A particularly interesting approach is to reduce the number of actuators without actually reducing the number of degrees of freedom [Birglen et al., 2008]. This approach, commonly referred as *underactuation*, bridges the needs of reducing the complexity of the control mechanism and improving the grasp of the hand.

Underactuated robotic hands are the middle point between full-blown robotic hands and simple grippers. By taking advantage of *mechanical intelligence* [Gosselin, 2006] embedded into the design of the hand allowing the shape adaptation of the fingers. Of further note is that underactuation in robotic fingers is different from the concept of underactuation as it is usually conceived in robotic systems. In the latter, it refers to a manipulator with one or more unactuated joints. On the other hand, underactuated robotic hands do have elastic elements embedded in their "unactuated" joints, that when combined with a suitable transmission mechanism, distribute an actuation torque or force to all joints [Birglen et al., 2008].

Underactuation in robotic hands generates intriguing properties that have only just begun to be studied. Although there has been abundant research in recent years into underactuated robotic hands, there is still a lot work left to do. Historically,

the *Soft Gripper* presented by [Hirose and Umetani, 1978] was the first prototype formally introducing the concept of underactuation. This *Soft Gripper* is a ten-phalanx two-finger gripper actuated by pulleys and cables. Notwithstanding that there are much older patents that take advantage of underactuation [Henning, 1919], the work done by Prof. Hirose is considered to be the cornerstone of underactuation in robotic fingers and the techniques presented are still in use today [Birglen et al., 2008].

Prosthetics is an application where underactuation can greatly extend the capabilities of existing systems without involving a complete redesign. In [de Visser and Herder, 2000], a prosthetic prototype is presented, having the important contributions of focusing the performance analysis on the contact forces of the finger rather than the kinematics, and the idea of a negative-stiffness spring mechanism to compensate the stiffness of the cosmetic glove.

An ideal grasping sequence has been taken for granted, even though it is not the case [Birglen et al., 2008]. Especially concerning underactuated robotic hands, an ideal grasping sequence is not always the case. In the literature available, the main corpus of knowledge of the theory behind the grasp properties of underactuated papers can be found in three references: two papers [Hirose and Umetani, 1978], [Shimojima et al., 1987] and one book [Birglen et al., 2008].

There have been many underactuated prototypes developed over the last twenty years. Table 1.1 presents a concise account of the most relevant underactuated prototypes present in the literature.

The development of underactuated mechanisms to be used as grippers, the use being as a prosthetic device or as the end-effector for a robot, has numerous examples. In Table 1.1 one can appreciate the different approaches taken by each research team.

Project	Driving Mechanism	Reference(s)
Soft Gripper (three-phalanx version)	Pulleys and cables	[Hirose and Umetani, 1978] [Greiner, 1990, Zecca et al., 2003]
Pinching gripper	Tendon-based	[Rovetta et al., 1982]
USC/Belgrade Hand	Rocker arm mechanism	[Rakic, 1989, Bekey et al., 1999]
Prosthetic hand	Linkage-based	[Crowder, 1991] [Dechev et al., 2001] [Kyberd et al., 2001] [Dubey and Crowder, 2002]
Prosthetic hand with elastic fingers	Tendon-driven	[Robinson and Davies, 1997] [Schulz et al., 2001] [Dilibal et al., 2002]
Prosthetic hand with compliant joints	Tendon-based	[Doshi et al., 1998] [Lotti and Vassura, 2002] [Ullmann et al., 2004] [Carrozza et al., 2005]
MARS Hand TUAT Hand	Linkage-based	[Gosselin and Laliberté, 1996] [Fukaya et al., 2000]
Prosthetic hand	Tendon-based	[Herder and de Visser, 2000] [Herder, 2001]
The *TAKO* gripper	Pneumatic bellows	[Yoshida and Nakanishi, 2001]
SARAH Hands	Planetary gear T-pipe circuit Linkage-based	[Laliberté and Gosselin, 2003]
Underactuated compliant gripper	Tendon-driven	[Lotti et al., 2005] [Dollar and Howe, 2006]
Underactuated compliant gripper	Linkage-based	[Boudreault and Gosselin, 2006]

Table 1.1 Underactuation prototypes found in the literature [Birglen et al., 2008].

An emerging trend is to use compliant joints in order to reduce the machining costs and the complexity of the mechanism.

In particular, [Boudreault, 2006] presents an underactuated compliant gripper made of Nitinol to be used in surgery. Although both this thesis and the latter reference share a similar objective, there are many substantive differences in their approach and results. First, the gripper presented in this thesis is not an adaptation of a previous design, but a complete redesign with five phalanges. Second, a finite element analysis (FEA) was done with the resulting optimized gripper in this paper. Third, the lifetime expectancy analysis of the finger is a new development never done in previous work. Finally, the sensitivity analysis done for the gripper presented here is also a new contribution with an underactuated compliant gripper.

CHAPTER 2

OUTLINE OF THE WORK DONE AND THESIS ORGANIZATION

Some authors have attributed the lack of success of robotic hands to the cost and complexity of these systems. Under-actuation offers a viable, cheaper alternative where robotic hands adapt themselves to the object being grasped by minimizing the driving input forces. In this case, a control law is not necessary and thus the complexity of the system is greatly reduced. The drawbacks of using a compliant architecture, which include the fragility of the mechanism and sometimes the instability of the gripping stance, are inherent problems in each design. A successful gripper was designed with those problems in mind and is presented here. It is also biocompatible thanks to the material used and could be used in surgery if developed further. The work done up until now is a large part of the effort required to develop an underactuated gripper for use in surgery, the foreseen changes required for the gripper to be used in surgery are a reduction of its size so it can fit in an incision as usually carried out in MIS and the addition of an remote actuation mechanism.

This thesis is based on a submitted article. The development of an underactuated gripper is described in its entirety in the aforementioned article. The research objective was to develop an underactuated gripper able to be used eventually in surgery and it was attained, with the results presented here. There are still some challenges ahead for the gripper to be used in surgery and they are discussed in Chapter 4. A prototype was created and several numerical simulations were made to analyze its expected performance.

The development of the gripper was done in several stages, they are presented in the order below.

1. Joint design.

2. Robotic finger design.

3. Optimization of the transmission mechanism for the robotic fingers.

4. Optimization of the driving mechanism.

5. Numerical simulations of the design.

All of the aforementioned stages are developed in Chapter 3. In the next Chapter there is a discussion of the results obtained as well as more details about the development of the gripper. Finally, the last Chapter presents the conclusion and possible future research directions.

CHAPTER 3

ARTICLE: DESIGN OF AN UNDERACTUATED COMPLIANT GRIPPER FOR SURGERY USING NITINOL

3.1 Abstract

This paper presents the development of an underactuated compliant gripper using a biocompatible super elastic alloy, namely Nitinol. This gripper has two fingers with five phalanges each and can be used as the end-effector of an endoscopic instrument. Optimization procedures are required to obtain the geometry of the transmission mechanism because of its underactuated nature and its underlying complexity. A driving mechanism further incorporated in the gripper to distribute actuation to both fingers and accomplish the grasping of asymmetrical objects without requiring supplementary inputs is also discussed. Finally, the results of numerical simulations with different materials and different grasped objects are presented and discussed.

3.2 Introduction

Surgery is one field that has been revolutionized by the use of minimally invasive surgery (MIS). It has allowed operations to be conducted through incisions of a few millimeters, using thin, flexible instruments with rigid end effectors [Kota et al., 2005]. Such procedures lead to shorter hospital stays, reduced costs, and less prominent scarring. In MIS, the development of end effectors that aid the surgeon by allowing a more effective grasp is highly desirable. This paper presents the development of an *underactuated* compliant gripper with better grasping capabilities.

This type of gripper has already been proposed in [Boudreault, 2006, Boudreault and Gosselin, 2006]. The latter authors developed an underactuated compliant gripper using Nitinol (NiTi), but there are many substantive differences between their approach and the one proposed in this paper. First, the gripper presented here is not an adaptation of a previous design, but a complete redesign with five phalanges and a new transmission mechanism. Second, a finite element analysis (FEA) was done to evaluate and optimize the life of the gripper.

Finally, a sensitivity analysis was carried out to estimate the effect of manufacturing tolerances or flaws on the theoretical performance of the gripper. It is a new development that has never been done with an underactuated or compliant gripper. Sensitivity analyses on underactuated grippers have been proposed in [Dollar and Howe, 2006], but they have focused on different aspects, namely the sensitivity of the performance of the finger due to variations in the joint torque ratio and compliance and not the impact of machining tolerances on performance.

Robotic fingers taking explicit advantage of underactuation have been proposed in the literature as far back as the 1970's [Birglen et al., 2008]. The first documented example is the *SoftGripper* [Hirose and Umetani, 1978], which used pulleys and was driven by cables. Another example of underactuated robotic hands are the SARAH prototypes [Laliberté and Gosselin, 2001] which were driven by linkages.

The underactuated compliant gripper presented in this paper is made out of Nitinol, a biocompatible alloy ideal for use in surgical tools. The gripper is ultimately envisioned to be used in laparascopic surgery, functioning above the austenite finish temperature where it exhibits its super elastic behavior. During its intended use, it will be subject to cyclic strains, and thus having an estimation of its usable life is important. The device is expected to present low-cycle fatigue because of the stresses in the mechanism will be high enough for plastic deformation to occur [Eiselstein,

2005] and therefore, a strain-life fatigue analysis is required. Promising results have been reported when using compliant mechanisms in surgical tools, especially due to the joint-free design and the possibility of force feedback [Kota et al., 2005].

Underactuated fingers have less actuators than degrees of freedom and rely on a transmission mechanism to distribute the input torque to the phalanges [Birglen et al., 2008]. Underactuation affords interesting capabilities to the fingers, allowing them to envelope an object without using a complex and costly control architecture. They are the intermediate solution between robotic hands for manipulation and simple grippers, as they take advantage of their shape-adaptation capability. They generally use elastic elements in the design of their driven joints. The transmission mechanism is composed of suitable mechanical elements like tendons [Hirose and Umetani, 1978], linkages [Gosselin and Laliberté, 1996], gears [Birglen and Gosselin, 2004a], etc., which distribute the actuation torque to the phalanx joints. The closing sequence of an underactuated finger is illustrated in Figure 3.1, where the spring keeps the shape of the linkage until the first phalanx of the finger makes contact with the object. As the actuation link continues to rotate, the second phalanx separates from the mechanical limit and the finger adapts itself to the object grasped.
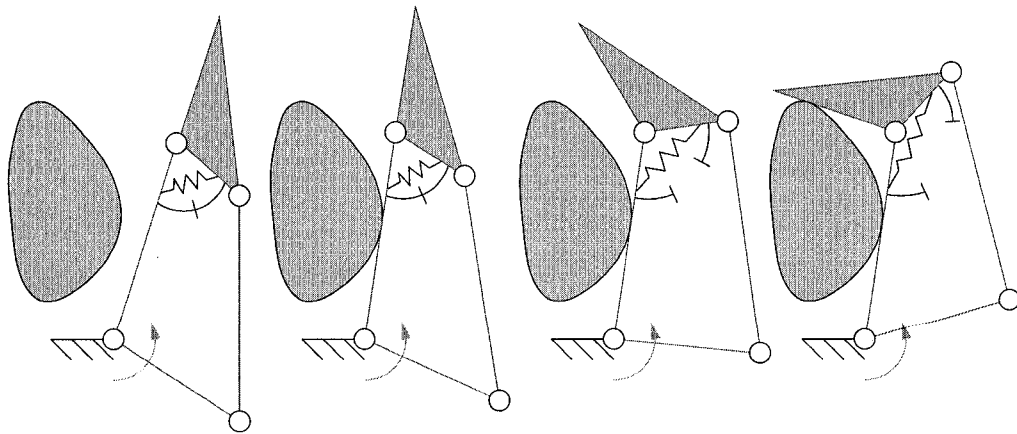
Figure 3.1 Closing sequence of a two-phalanx underactuated finger [Birglen et al., 2008].

Drawing on the previous work of the authors [Birglen, 2006, Birglen et al., 2008], the transmission mechanism of the compliant gripper presented here has received close attention. Different architectures were tested, but given the material constraints (permissible stress, strain), fabrication constraints (minimum widths, etc), external loads, and desired performance, many of them had to be discarded. Furthermore, the analysis of the driving mechanism converting a linear input force into an input torque for the fingers was optimized separately to simplify the design process. In [Birglen, 2006], an introduction to the analysis of underactuated fingers is presented using a two-phalanx finger as an example. As the number of phalanges increases, the complexity of the analysis grows exponentially and the usable workspace defined by having all-positive contact forces might decrease drastically. The fingers of this gripper have five phalanges and thus may have a very small workspace if improperly designed.

3.3 Joint Design

The gripper design starts with the robotic fingers. Their length was chosen to be close to the one from some common laparoscopic pincers [Intuitive Surgical, 2008b]. Nitinol was chosen to constitute the gripper because of its biocompatibility and super elastic properties, allowing the joints to have a large range of motion and to be used in surgery without additional coating. A wire cut electrical discharge machining (EDM) process can be used to manufacture NiTi parts but it imposes a minimum joint thickness. In this case, to avoid performance issues like deformation of links outside of the joints or a reduced lifetime because of joints being too thin, the minimal joint thickness is set to 0.25 mm. The shape of the hinge joints is inspired by [de Bona and Munteanu, 2005]. A corner-filleted flexure hinge has very good compliance for single-axis use, both in the symmetric and non symmetric

cases [Lobontiu, 2002]. Both types of joint were modeled and optimized using a Design of Experiments method [Montgomery, 2005] with a FEM commercial software, where infinite life was considered at 10^3 flexures as reported in the low-cycle fatigue data in [Wilkes and Liaw, 2000]. The desired maximum rotation of the joints is 70°. By using a filleted flexure hinge, the life of the joint is increased since there are less stress concentration points. The results show the maximal lifetime for the asymmetrical joint is achieved with a fillet-radius of 0.30 mm, and for the symmetrical joint with a fillet-radius of 0.4 mm. The resulting joints are illustrated in Figure 3.2.

(a) Optimized asymmetrical joint   (b) Optimized symmetrical joint
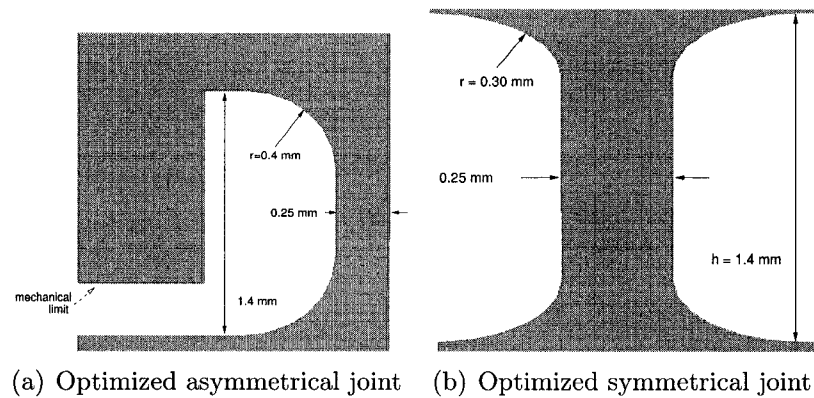
Figure 3.2 Joints used in the finger.

Asymmetrical joints have been considered to avoid a foreign object getting lodged in the joints between the phalanges contacting the object seized, and thus, possibly damaging biological tissue. Mechanical limits are included in these joints to prevent them from rotating in an undesired direction. For the symmetrical joint, the fillet-radius of 0.30 mm was chosen because it produces an acceptable lifetime for the device and by increasing the compliance of the joint, it reduces the force needed to drive the gripper.

(a) Asymmetrical joint

(b) Symmetrical joint
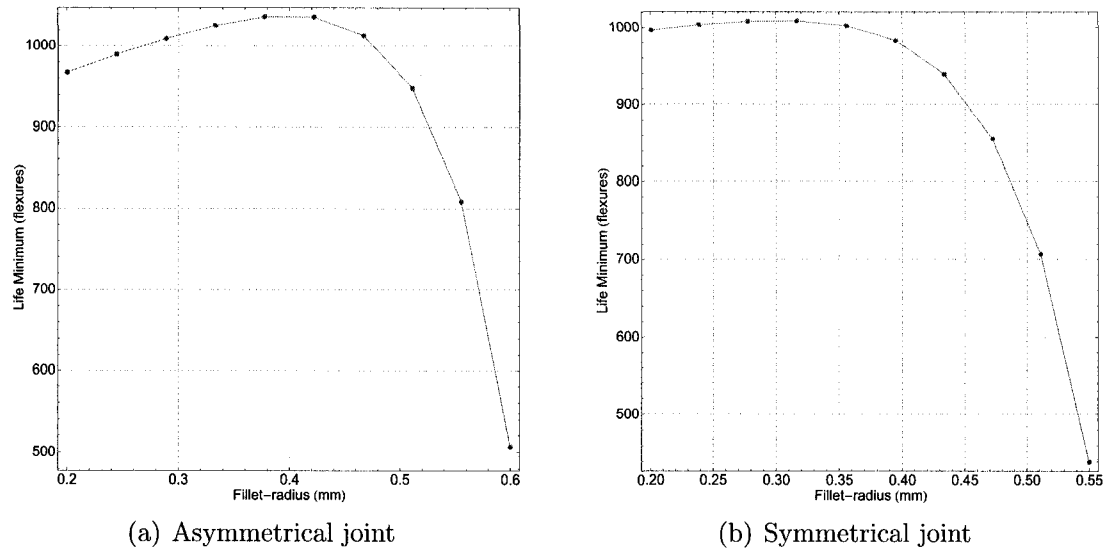
Figure 3.3 Lifetime of the joints as a function of the corner-fillet radius.

3.4 Underactuated Finger Design

Underactuated fingers can be analyzed as the connection of robotic fingers plus several differential mechanisms driving their joints which results in a self-adaptive capability [Birglen et al., 2008]. A finger with five phalanges was chosen in order to have a large adaptability and to reduce the rotation demanded from each individual joint, thereby increasing the lifetime of the device. The length of each phalanx was decided to be 5 mm and of each joint to be 1.4 mm long. These considerations bring the length of the finger (32 mm) in line with some common laparoscopic pincers. Regarding the driving mechanism, it is composed of a transmission mechanism distributing the actuation torque to the phalanges, and a base mechanism converting a linear force into the input torques for the fingers (cf. Figure 3.4). The objective of the transmission mechanism is to drive the finger as it grasps an object. It must continue to distribute force as each phalanx of the finger touches the object, losing a degree of freedom (DOF). Several architectures are possible for this task and three mechanisms were chosen to be compared.
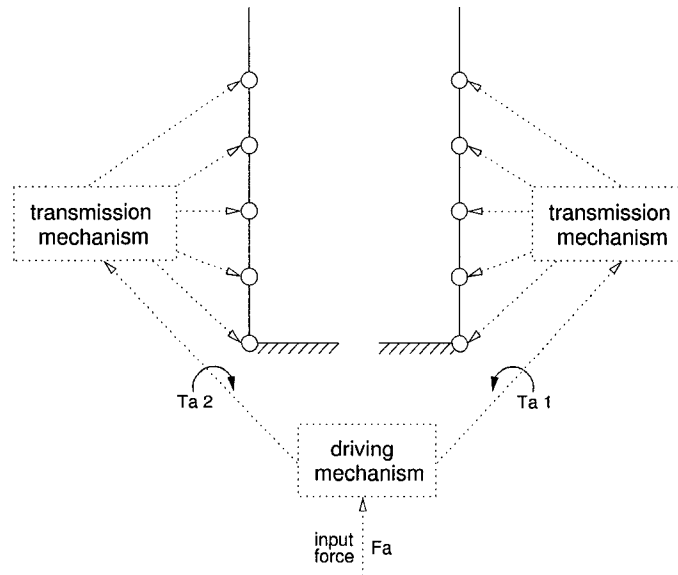
Figure 3.4 Division of the constitutive mechanisms of the gripper.

The use of compliant joints demands the rotation of the joints to be as even as possible, distributing the deformations to as many joints as possible to increase the life of the device. The first architecture considered (Figure 3.5(a)) consists of a five-bar linkage [Birglen and Gosselin, 2004b] where the proximal phalanx is subdivided into four phalanges. Each division generates a new DOF. The second architecture (Figure 3.5(b)) is a three-stage mechanism inspired by the work presented in [Gosselin and Laliberté, 1996]. It is a good compromise between a four-stage mechanism with a better deformation distribution, and the force required to drive the finger. The third and final architecture is a modification of a five-bar linkage with a four-bar linkage in the middle to decrease the range of motion required in the joints of the transmission mechanism of the former case.

The distribution of contact forces once an object has been contacted is much more relevant than the movement of the finger before the grasp [Herder and de Visser, 2000] and is therefore the main concern in the design. A method to obtain the analytical expressions of the contact forces of underactuated fingers is presented

(a) Architecture 1 (b) Architecture 2 (c) Architecture 3
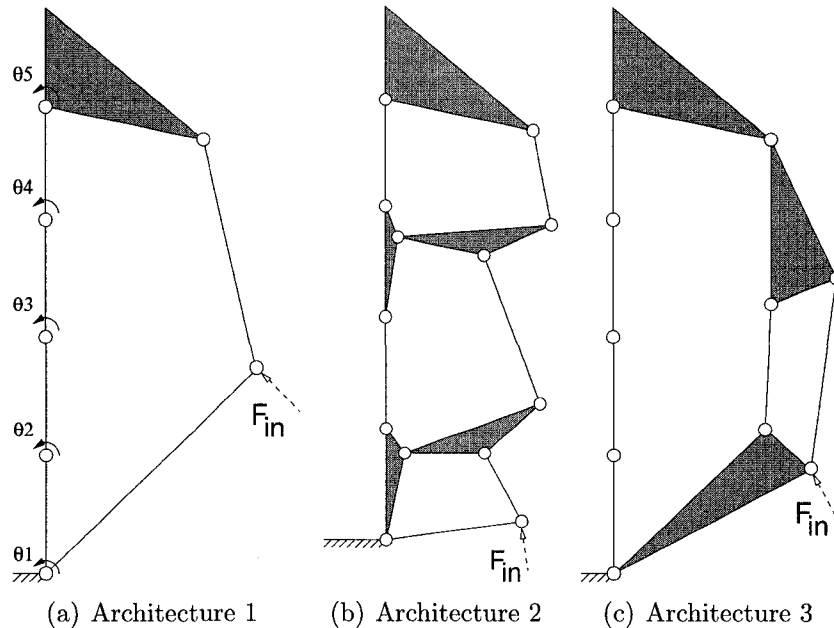
Figure 3.5 Finger architectures considered.

in [Birglen et al., 2008] and has been extended to compliant cases in [Birglen, 2006]. The *Transmission and Jacobean matrices* presented in these references are valuable tools to envision the performance of the finger. Similarly, contact forces can be obtained with a static analysis which is preferable in the compliant case due to the complexity of the latter matrices. Taking into account five contact forces, the following linear system is obtained:

$$\mathbf{G}\mathbf{f} = \mathbf{k} \qquad (3.1)$$

where $\mathbf{k}$ is a vector containing the elastic torques generated by the compliance of the joints [Birglen, 2006], matrix $\mathbf{G}$ is obtained by combining the equations derived from the static equilibrium of the finger, and vector $\mathbf{f}$ contains the contact forces

$(\mathbf{f_c} = [F_1 \ldots F_5]^T)$ and the internal forces of the mechanism $(\mathbf{f_i})$, i.e.,

$$
\mathbf{f} = \begin{bmatrix} \mathbf{f_c} \\ \mathbf{f_i} \end{bmatrix}, \mathbf{k} = \begin{bmatrix} \mathbf{0} \\ \mathbf{t} \end{bmatrix}, \mathbf{t} = \begin{bmatrix} T_a \\ T_1 = -k_1 \Delta\theta_1 \\ T_2 = -k_2 \Delta\theta_2 \\ \ldots \\ T_n = -k_n \Delta\theta_n \end{bmatrix} \tag{3.2}
$$

where k_i is the stiffness of the compliant joint associated with θ_i [Birglen, 2006], and n is the number of compliant joints in the finger. Solving eq. (3.2) allows to compute the force vector $\mathbf{f}$, namely,

$$
\mathbf{f} = \mathbf{G}^{-1}\mathbf{k} = \mathbf{G}^{-1} \begin{bmatrix} \mathbf{0} \\ \mathbf{t} \end{bmatrix} \tag{3.3}
$$

3.5   Optimization of the Transmission Mechanism

3.5.1   Introduction

The objective of this optimization procedure is to obtain the geometric parameters that will be used in the transmission mechanism of the fingers. These geometric parameters define the performance of the gripper inside its workspace. Each joint has a range of motion of 45°, lower than the designed limits of the joints to further increase the lifetime of the gripper. Considering the large number of parameters to be taken into account, the optimization was done using a genetic algorithm (GA). Basic parameters for the latter were based on Dejong's settings [DeJong and Spears, 1990]. The population size and the crossover fraction were further refined by a deterministic study where a range of values for each of the parameters were tested against a function representing a five-phalanx underactuated finger using a

three-stage transmission architecture. Because the genetic algorithm is a stochastic system, a Monte Carlo analysis was done with 10 iterations. Figure 3.6 shows a marked improvement in the average results by increasing the population size and by reducing the crossover fraction compared to the recommended values. The fitness function is described in detail in the following section.

(a) Population size

(b) Crossover fraction
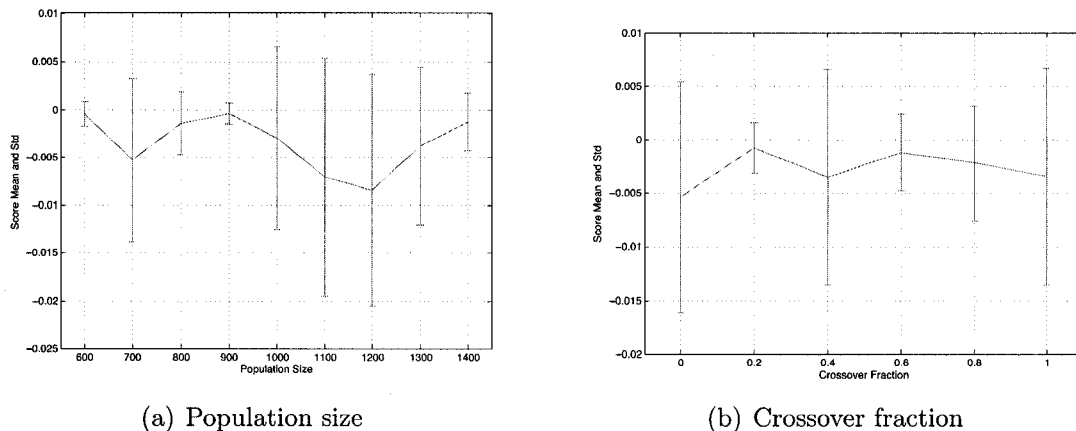
Figure 3.6 Fine-tuning of the GA parameters.

3.5.2   Grading function

When using an index to grade the performance of a transmission mechanism, the finger is optimized to perform well under a certain metric. If the optimization metric does not favor the desired usage, the resulting gripper will underperform. The first attempt at optimizing this gripper had a global approach, where the resulting mechanism would perform well throughout the whole workspace. In reality this method is not the best suited as it does not favor the most common cases, and thus a localized approach was chosen by developing particular test cases or objects.

A grading or fitness function assigns an index to each design. Given the geometric parameters and five angles $(\theta_1, \ldots, \theta_5)$ that define a grasp, it evaluates the perfor-

mance of the finger in this particular situation. First of all, this function requires the following conditions:

1. All contact forces are *positive*. This is required to have a stable grasp [Birglen and Gosselin, 2003, Birglen and Gosselin, 2006d].

2. The torque acting on the last phalanx must not be negative.

3. The projection on the last phalanx of the intersection between both lines associated with the links attached to this last phalanx is *inside* the latter [Laliberté and Gosselin, 2001].

4. When using a test object, the resultant force applied on this object pushes the latter towards the palm of the gripper.

A design passing all of the aforementioned tests is then graded using the following indices:

1. *Deformation*: the maximum deformation in the joints is compared to the maximal value allowed. The lower the deformation, the higher the score:

$$m_d = \frac{45°}{\text{largest deformation}} \qquad (3.4)$$

2. *Force multiplication*: all the contact forces are added and divided by the input force (cf. Figure 3.5). This index favors designs generating a force on the grasped object close to the input force:

$$m_{fm} = \frac{\sum_{i=1}^{5} F_i}{F_{in}} \qquad (3.5)$$

3. *Force isotropy*: the standard deviation (σ) of the forces allows us to characterize the uniformity of the grasp; a smaller standard deviation indicates

a uniform pressure of the finger. This rewards force-isotropic [Birglen and Gosselin, 2004b] designs and is desired in order to avoid large local forces on the object:

$$m_{fi} = 1 - \frac{\sigma(\mathbf{f_c})}{\sigma(\mathbf{f_c}) + 5} \qquad (3.6)$$

Finally, these indices are multiplied together to obtain a grade for the finger with the given parameters and position:

$$\text{Grade} = m_d \, m_{fm} \, m_{fi} \qquad (3.7)$$

3.5.3 Optimization Process

Each set of geometric parameters (candidate) is evaluated with the grading function defined by eq. (3.7). Test objects were also chosen, considering that the gripper is believed to grasp objects with shapes close to a circle. Examples of these test cases are illustrated in Figure 3.7. In the optimization process, the radius of the circle representing an object being grasped ranges from 7 mm to 25.2 mm.

First, the candidate are evaluated with the test objects and their grades are averaged. Second, the candidate is further scrutinized by analyzing how well it would perform when only θ_1 and θ_5 are allowed to move ($\theta_2 = \theta_3 = \theta_4 = 0$) which allows to test the grasping of an object when most of the finger is locked and rewards designs that allow the last phalanx to close even if the rest of the phalanges are immobile, e.g., when grasping a very large object. Finally, it checks the proposed candidate over the whole workspace, defined by the angles $\theta_i \in [0, 45°]$ with $i = 1, \ldots, 5$, to insure that the deformation constraint is respected. The final *global* grade of the candidate is composed of:
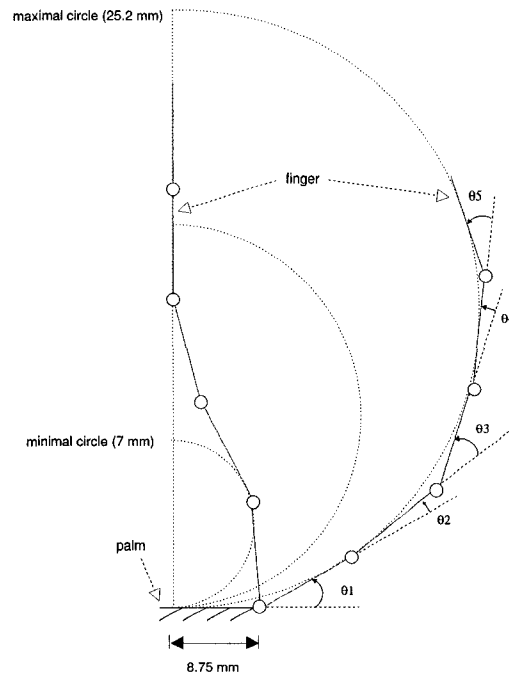
Figure 3.7 Examples of test objects used in the optimization.

1. the average of the grades received by evaluating the candidate with the test objects $(\bar{x}_T)$.

2. the average of the grades received by evaluating the candidate when only θ_1 and θ_5 are allowed to change $(\bar{x}_L)$.

3. the average of the grades received by evaluating the candidate over the whole workspace $(\bar{x}_W)$.

Together, these elements are combined with different weights serving as the fitness function of the GA:

$$\text{Mechanism Grade} = 10\,\bar{x}_T + 3\,\bar{x}_L + \bar{x}_W \qquad (3.8)$$

The grading function defined above has many different local minima. Given that

the probability of not finding the global minimum of this function is not negligible [Rudolph, 1994], the GA was repeatedly run to collect various local minima and then compare the three architectures considered. Figure 3.8 shows a box plot of the results of the GA runs with the three different architectures where one can appreciate the large variation between results and the large number of outlier values which are better performing geometric parameters and thus more desirable targets. These results suggest a large sensibility of the optimization process to small changes in the geometric parameters. Statistics of the grades are shown in Table 3.1.
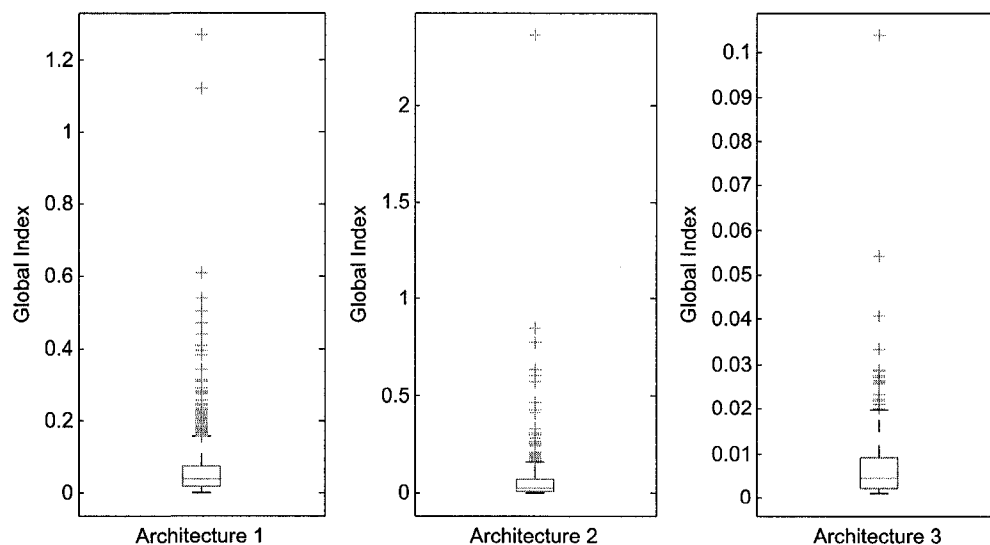
Figure 3.8 Box plots of the optimization results.

Architecture	1	2	3
Average grade (10^{-2})	6.28	7.12	0.83
Maximal grade	1.2697	2.3609	0.1040
Minimal grade	0.0015	0.0011	0.0010
Standard deviation	0.0898	0.1881	0.0879
Variance (10^{-2})	0.81	3.54	0.01514

Table 3.1 Comparison of the three finger architectures.

The results were interesting and in particular, architecture 3 (cf. Figure 3.5(c)) showed potential regarding its capability to envelope the finger around an object.

However, two revolute joints must accommodate a very large range of motion which is impractical with the joint design proposed here. To give room to such movement, the joint lengths would have to be excessively large and become a possible point of failure for the finger. In conclusion, architecture 2 (cf. Figure 3.9), having the highest average and performance score, was selected as the transmission mechanism. The geometric parameters of the finger are presented in Table 3.2 with reference to Figure 3.9, note that lengths d_1 and d_2 are set to 1 mm, their minimal value.
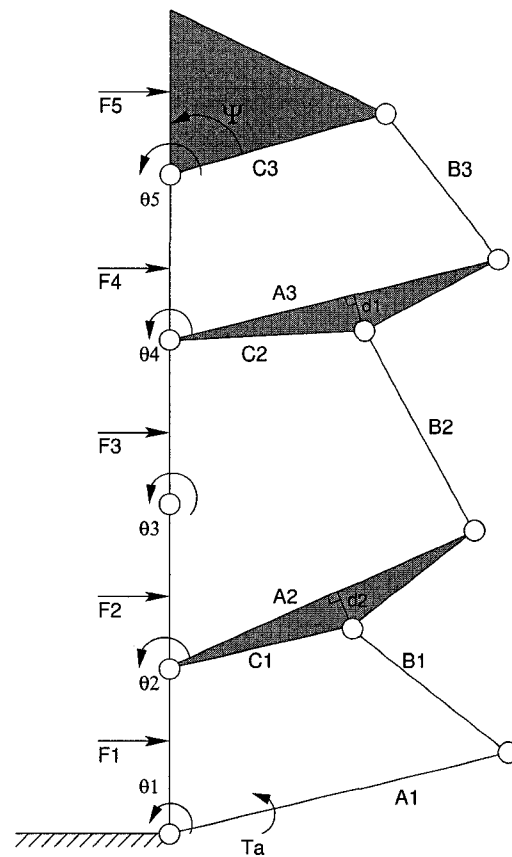
Figure 3.9 Three-stage driving mechanism architecture used.

$\mathbf{A_1}$	$\mathbf{B_1}$	$\mathbf{C_1}$	$\mathbf{A_2}$	$\mathbf{B_2}$	$\mathbf{C_2}$	$\mathbf{A_3}$	$\mathbf{B_3}$	$\mathbf{C_3}$	Ψ
15.7	18.4	9.1	13.4	12.9	3.4	14.7	14.2	7.5	83°

Table 3.2 Geometric parameters of the finger (mm).

3.5.4 Sensitivity Analysis

To ensure that the finger has an acceptable performance when manufactured, the effects of manufacturing tolerances on the design have to be analyzed. A factorial approach is used because it a statistically correct approach when dealing with many factors (i.e., the geometric parameters of the finger) and looking for possible interactions between them [Montgomery, 2005]. The analysis of variance (ANOVA) [Montgomery, 2005] tests the effects of multiple factors on the mean of the grade; it subdivides the total variation into variation due to main factors, variation due to interacting factors, and variation due to error. This study assumes that the sample populations are normally distributed. There was only one repetition of the experiment since there is no external noise in the system as the results come from eq. (3.8) and only depend on the input parameters. In this study, the statistically significant factors and interactions affecting the performance of the fingers due to manufacturing tolerances are determined using a 2^{10} factorial design with two-level treatments. Subsequently, a 8-way ANOVA is carried out with the results. The high level of the factors was set to an increase of 0.2 mm or 2° in the geometric parameters, and the low level was set to a reduction of 0.2 mm or 2°, representing the tolerance of the EDM manufacturing process.

A normal probability plot of the residuals of the 8-way ANOVA is shown in Figure 3.10. Although the bulk of the observations form a straight line, implying a normal distribution, there is a small number of points deviating from it. The ANOVA revealed 295 statistically relevant interactions ($p < 0.05$), and that the factors A_2, A_3, B_3, C_3 alone are statistically significant. The p-value is the probability that the difference between groups during the experiments happened by chance [Dean and Voss, 1999]. When it is lower than the significance level, $\alpha = 0.05$, the factor or interaction is considered to be statistically significant. The large number of sta-

tistically significant interactions leads us to conclude that the performance of the gripper will be very sensitive to manufacturing defects.

This result is in accordance with the sensitivity illustrated in the box plot of architecture 2 (cf. Figure 3.8), where there is a set of geometric parameters which stands out and is far away from the mean. Finally, the results should be taken in context and remember that the global grading function (3.8) is limited in the sense that it returns a value of zero if any contact force is negative. In practice, this may not be disastrous to the performance of the finger as it will continue to adapt itself to the object. Ejection of the object is possible [Birglen et al., 2008] but given the limited workspace imposed by the substantial number of phalanges, the criteria used to evaluate the fingers based on the contact forces is believed to be accurate.
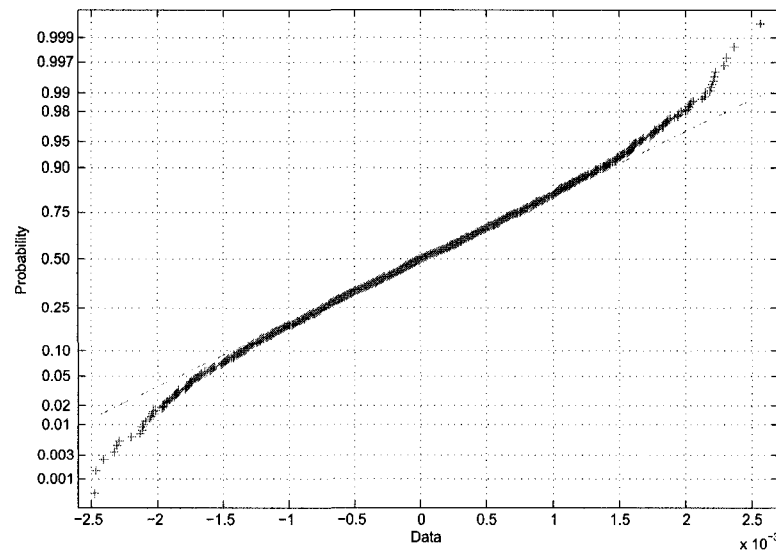
Figure 3.10 Normal probability plot of the residuals of the ANOVA.

3.6 Optimization of the Driving Mechanism

The driving mechanism converts a linear actuation force commonly used in MIS into input torques for both fingers. Furthermore, when grasping an asymmetrical object, it must transfer more torque to the finger that did not fully close, intending to bring the object towards the center of the palm. For example, if a finger lags behind the other during its closing motion, the driving mechanism has to direct more torque towards this finger. It should also maximize the torque delivered to the transmission mechanism. Finally, the deformation in its joints should also be minimized. This driving mechanism is modeled after a seesaw mechanism [Birglen and Gosselin, 2006a]. The mechanism is optimized taking into account the criteria mentioned before while also considering the size and machining constraints.
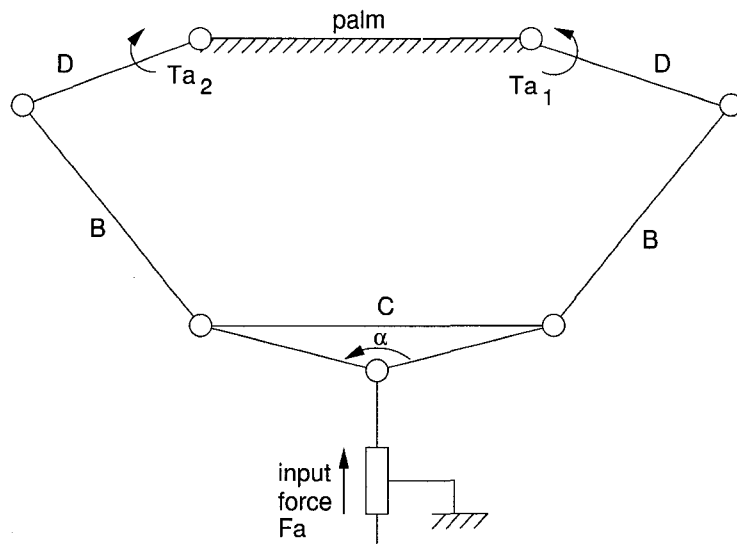
Figure 3.11 Seesaw driving mechanism.

As noted in [Boudreault, 2006], for the mechanism to properly balance the output torques, the seesaw link (cf. Figure 3.11) should have the shape of a triangle with

angle α greater than 180°. The following index is used as the performance index:

$$\delta_d \left(\frac{|T_{a1} - T_{a2}|}{\text{largest torque in the workspace}} \right) \tag{3.9}$$

where δ_d has a value of 0 for the finger that lags behind if it receives less torque than the other, or else a value of 1. The volume of the surface generated by the index defined by eq. (3.9) when it is calculated over the whole mechanism workspace is used as the fitness function of a GA again. This surface is illustrated in Figure 3.12 for the geometric parameters of the driving mechanism presented in Table 3.3 which correspond to the result of the optimization.

D	B	C	α
16.3	25.88	31.56	252°

Table 3.3 Geometric parameters of the driving mechanism (mm).
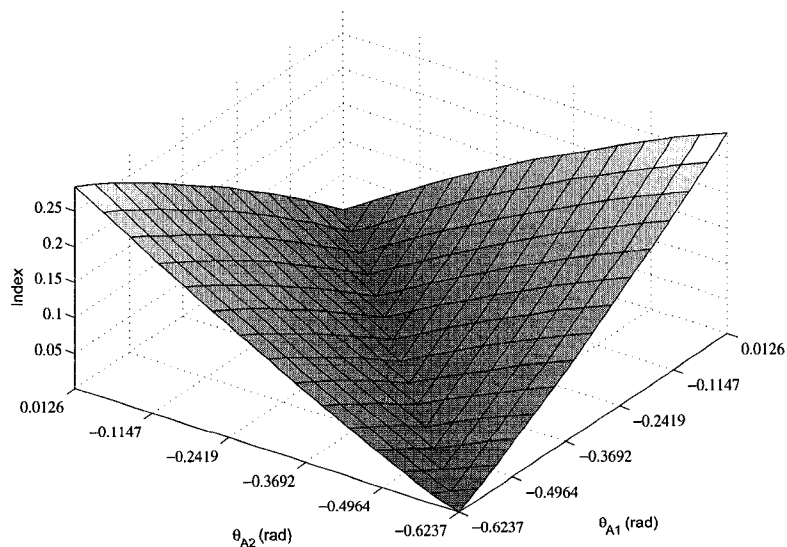
Figure 3.12 Performance index of the driving mechanism.

Finally, a relationship between the length of the finger and the palm reported in [Laliberté and Gosselin, 1998] was considered during this optimization. Taking the suggestions proposed along with size constraints, a 0.545 palm/finger ratio was chosen.

The finger length being 32 mm (it includes five phalanges and five flexural joints), the palm length is 17.5 mm. With the finger, driving and transmission mechanisms determined, a final design is obtained, illustrated in Figure 3.13 and a prototype is shown in Figure 3.14.
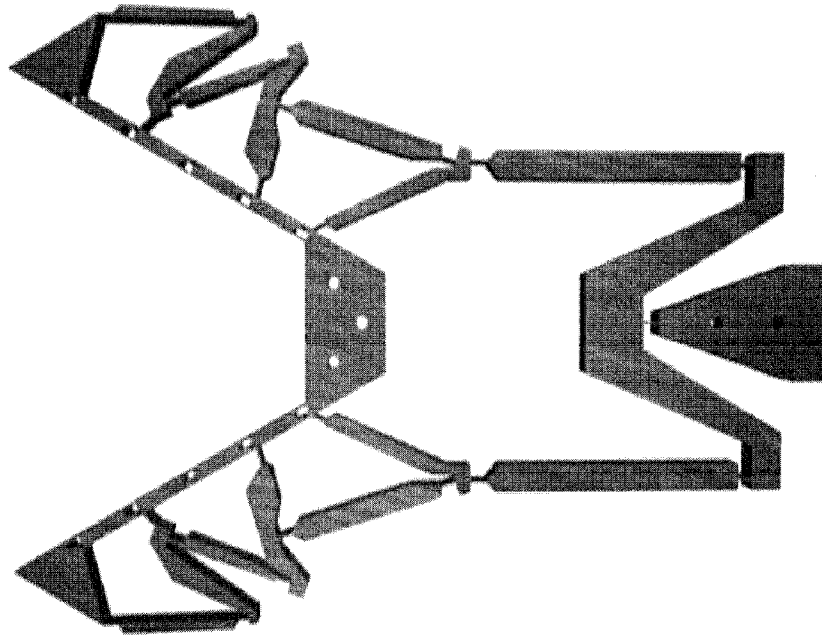
Figure 3.13 Optimized final design.

3.7 Finite Element Simulation

A finite element simulation was done using a commercial FEM software to validate the final design obtained. The software has a shape memory alloy (SMA) module which allows it to give an accurate simulation of how an actual prototype would behave because it takes into consideration the super elastic properties of Nitinol. To the best of the authors' knowledge, it is the first time that this is done with an underactuated compliant gripper. To compare and highlight the usefulness of
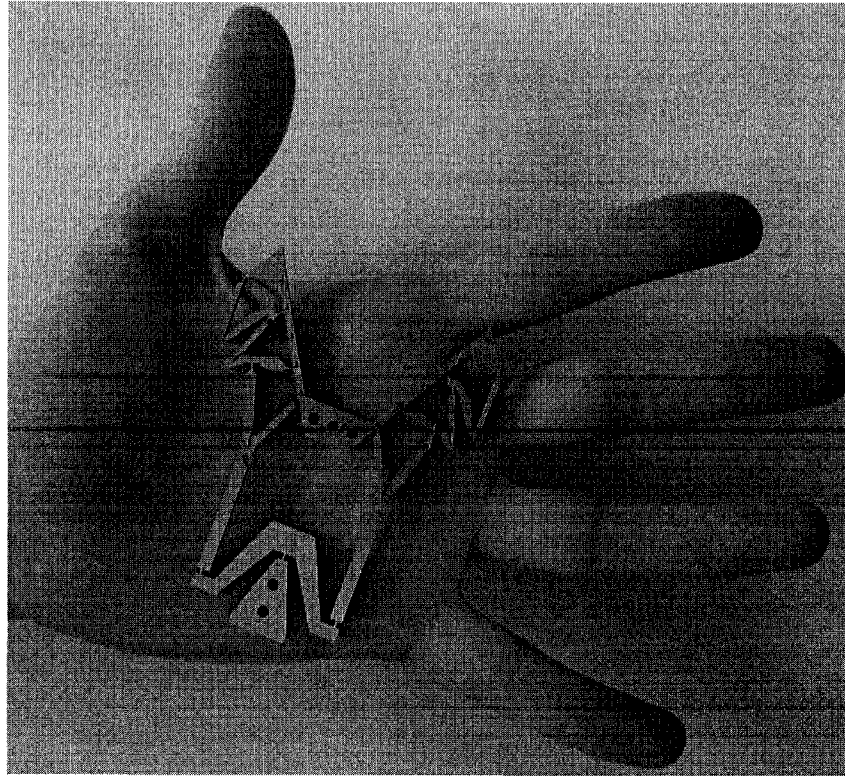
Figure 3.14 Prototype of the gripper.

Nitinol, the same simulations were performed using four other different materials: aluminum alloy, 316L stainless steel, polypropylene, and ABS plastic [MatWeb, 2008]. Results are illustrated in Figs. 3.15 and 3.16. The results are promising and show that the gripper can envelope and secure different objects of various shapes. For the case shown in Figure 3.15, the base of the gripper required a displacement of 7 mm and has an expected lifetime of 982 flexures. The required force to grasp an object and the maximum Von Mises stress is reported in Table 3.4.

Material	Nitinol	Steel 316L	ABS Plastic	Poly-propylene	Aluminum
Required driving force (N)	79	1110.6	16.5	10.4	390.1
Maximum Von Mises Stress (MPa)	1405	32527	409	265	11303

Table 3.4 Force needed to drive the gripper using different materials.

3.8 Conclusion

This paper underlines the versatility offered by the use of compliant underactuated grippers using Nitinol. The use of such end-effectors in laparoscopic surgeries is an exciting avenue of opportunity where the onus of the grasping motion is shifted away from the control electronics to an intelligent mechanism.

The development of a gripper was presented which substantiates the feasibility of the use of underactuated compliant grippers. Special attention was paid to the selection and optimization of the transmission mechanism, with a focus on finding a set of geometric parameters that allows the fingers to perform satisfactorily under all circumstances. The results obtained were validated using a FEM software which took into account the super elastic properties of the material.

Further validation of the simulation results should be done, as the results reported here are only based on numerical simulations. Part of the continuing work shall include destructive testing to confirm the lifetime expectancy analysis and possible consequences of the manufacturing process. The sensitivity analysis presented here relied on a statistical method an often used in other fields which was applied successfully to the development of an underactuated compliant gripper. This development process has indicated that the optimization criteria based on the contact forces is valid but very stringent when the number of phalanges is large.

3.9 Acknowledgements
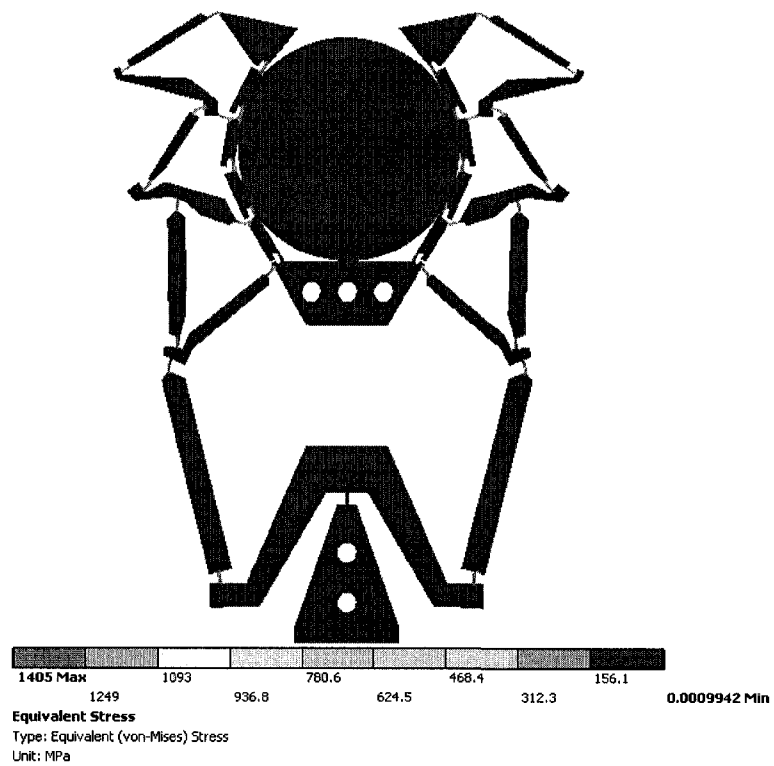
Figure 3.15 Von Mises stress of a Nitinol gripper during a symmetrical grip.

34
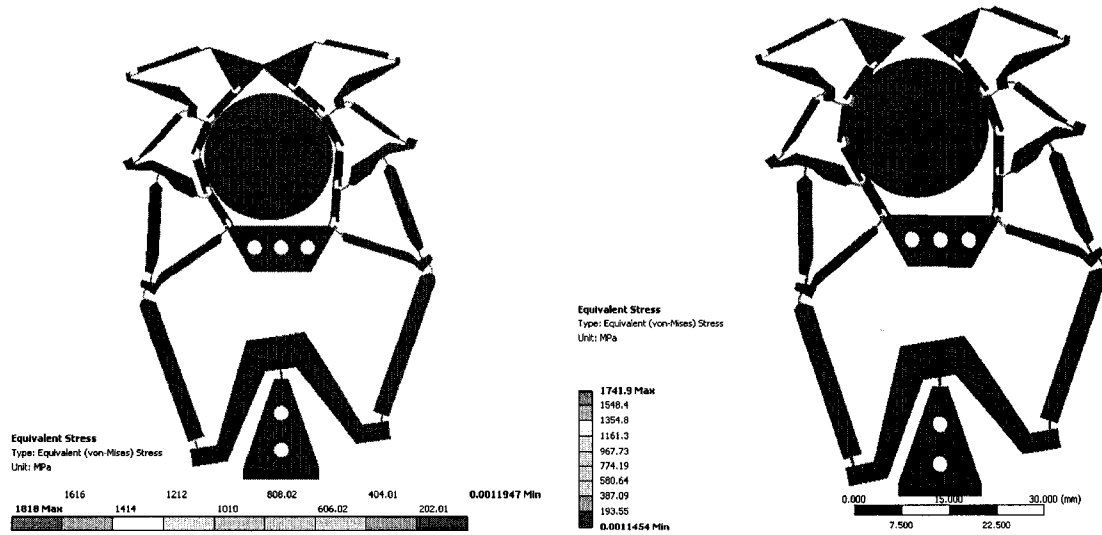
Figure 3.16 Von Mises stress of a Nitinol gripper during an asymmetrical grip.
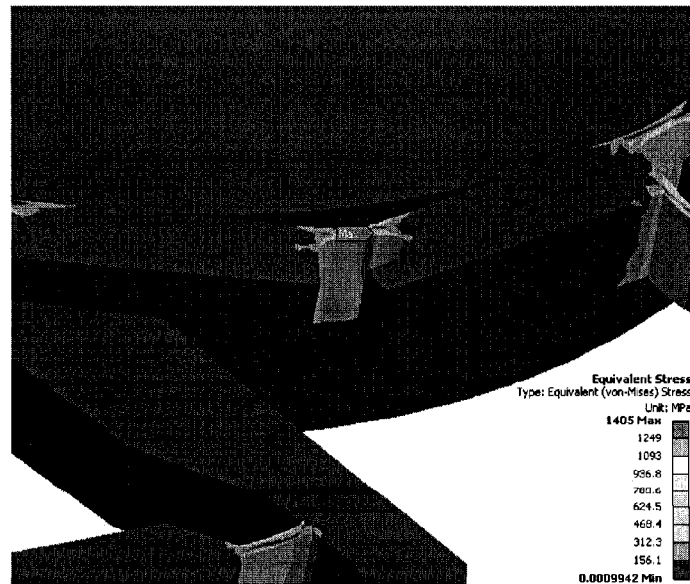
Figure 3.17 Close-up of the most solicited joint of the gripper using Nitinol.

CHAPTER 4

GENERAL DISCUSSION

This thesis presents the work done to develop an underactuated compliant gripper using Nitinol. In the preceding chapter, the article submitted to the ASME Journal of Medical Devices detailing the work was shown. In the literature review one can appreciate the large quantity of prototypes in existence but the theoretical work that can be used as guidelines in their design is still shallow. Yet, there are many successful grippers for very different uses, and most of them have been developed following the example of previous grippers. Up until very recently, few new theories were presented. They are very welcome and present a path on how to create better grippers without resorting to a costly cycle of designing, building and testing a prototype.

The gripper presented was optimized with a focus on the mechanical aspects of its performance. It was the intention of this work to test the theories available to verify their conclusions. Although the gripper is envisioned for eventual use in minimally invasive surgery, the optimization criteria included few elements related to surgery. The size of the robotic fingers was limited to resemble a commercial surgical manipulator (e.g, [Intuitive Surgical, 2008b]) and the optimization process penalized designs that became too bulky. The gripper might have problems to fit inside an endoscopic tube, but it could be compressed by taking advantage of its super elastic behavior in order to make it fit. This is an area of continuous work and further studies could continue in this direction. Another alternative would be to design a smaller gripper with less phalanges, using the conclusions and optimization process used in the development of this gripper.

The idea behind the joint design was to maximize the life of the gripper. In a previous gripper [Boudreault, 2006], it was reported that the manufacturing of the joints was difficult because their width was very small and the electrical discharge machining process could hardly produce them. Making the joints wider was a necessity but also implies that the actuating force of the gripper will be considerably higher. Another consideration to have when producing the gripper was the thickness of the Nitinol sheet, the supplier (Johnson Mattey Metals) expressed that they usually do not produce Nitinol with the thickness demanded.

Many more architectures were studied but they were not mentioned in the article. A basic analysis was made on them by simulating their transmission mechanism and looking for obvious problems, like the inability to grasp an object or if there were any links that would collide between them before the finger could finish its grasping motion. Architecture 1 (see Figure 3.5(a)) is the simplest mechanism one can have for a linkage-driven finger. One can see that it can be regarded as a two-phalanx finger (see Figure 3.1) with the proximal phalanx divided into four parts. This is interesting because this new finger with five phalanges could offer a better theoretical distribution of force around the object (five contact forces instead of two) and would provide a simple way for increasing the adaptability of a mechanism. The problem observed is that because the transmission mechanism is only in contact with the distal phalanx, the mechanism behaves as if it were enveloping the object with the phalanxes, and thus can easily develop negative contact forces. The architecture chosen, architecture 2 (see Figure 3.5(b)), does away with this problem by providing support on the first, third, and fifth phalanges. Also, during tests the phalanges that were most likely to develop a negative contact force were the ones that did not receive a direct support from the transmission mechanism. In this case, phalanges two and four can thus be seen as adaptability enhancers, allowing the robotic finger to offer better grasping capabilities than a three-phalanx finger with support on

each phalanx from the transmission mechanism.

As noted in [Laliberté and Gosselin, 2001], the condition that lengths C_i in the transmission mechanism must be as small as possible holds true, as shown in Figure 3.9. Even though the optimization was carried out using a genetic algorithm, the results concur and show that lengths C_i are usually at their lower limit in the resulting mechanisms.

When analyzing how a set of geometric parameters would behave given a test object, the objective was to characterize the performance of the finger when grasping both big and small circular objects. It is relevant to note that to grasp small circular objects, the finger will grasp it requiring only two phalanges and the rest will not be used. To take advantage of symmetry, it was considered that the rest of the phalanges would make contact with each other, giving the gripper a form as if it was pinching an object. The results are interesting and deserver further development, as they assume that there is only one contact force between the fingers and that it happens in the middle of the phalanx. This is a simplified model that does not take into account if the finger could actually reach that position. Furthermore, without a theoretical description of the path followed by the finger which for the moment requires an expensive numerical analysis (detailed FEM simulation), predicting the final position of the finger when grasping a small object is not feasible. A theoretical model would required detailed mechanism equations and a good model of the compliant joints. When exploiting the super elastic capabilities of Nitinol, this analysis would become onerous and would dispense with the advantages offered by theoretical model available at the moment.

The objective of the driving mechanism is to convert a linear actuation force, as one could find in a linear actuator used in a laparoscopic pincer to open and close it, into two torques that close the robotic fingers of the gripper. The driving mech-

anism optimization was carried out using a genetic algorithm with an index which characterized the performance of each candidate mechanism. This index gives a positive grade (> 0) only if when both angles ($\theta_{1,2}$) are equal, their respective links generate equal closing torques, and when the angles are different, the link with the smaller angle generates a greater torque. The best parameters are shown in Table 3.3. Figure 3.12 shows the result of the optimization, where the lower axes of the graphic depict the angles $\theta_{1,2}$ as they move in the workspace; when they are not equal, the index should be greater than zero, and the resulting graphic should be symmetric.

The use of ANOVA in this thesis is a new development that to the best of the author's knowledge has not been used before with underactuated fingers. It underlines the sensitivity of the optimization function to small changes in the geometric parameters of the finger. At the beginning, the use of ANOVA was envisioned as a sensitivity measure; by increasing the experiment by a small amount and then doing an analysis of variance on the results, one can find the point where there is statistical evidence that the quality of the gripper will change. In the case of the gripper presented here, even the manufacturing tolerances showed an effect on the theoretical performance of the gripper.

Finally, concerning the finite element simulations, the commercial package *ANSYS* was used because it includes a module to simulate shape memory alloys. The fatigue information about Nitinol was based in [Eiselstein, 2005]. It was considered to be above its austenite finish temperature, in this case greater than 29°C. The simulated grasped object was fixed and used a stainless steel material, making it much harder than the gripper. Finally, because of the non-linearities introduced by the contact between the two objects and the super elasticity of Nitinol, the base of the gripper was actuated with a displacement instead of a force.

CONCLUSION AND RECOMMENDATIONS

Chapter 3 presented the development of a compliant underactuated gripper using Nitinol. The results obtained from the FEM simulation are encouraging and showed a gripper that can adapt itself to different objects and grasp them successfully. The force needed to actuate the gripper is large as expected due to the thickness of the joints and implies that the closing force must be provided by an (electrical) actuator. The thickness of the joint was a limitation imposed by the EDM process. By reducing it, the force to actuate the gripper decreases drastically.

The optimization of the finger was done using a genetic algorithm whose fitness function can drop to zero very easily, suffice it for any of the contact forces on the finger to become negative for this function to be zero. In reality, a negative force does not necessarily cause a faulty grasp, merely one where some of the phalanges are not in contact with the object. While testing the finger, three of the five phalanges would usually be positive, giving the impression that the two phalanges left are just working as supports for the rest of the phalanges. They do not contribute towards grasping the object but instead allow the other three phalanges to have a better position from where to grasp the object. The theoretical framework available is very useful in guiding the design of the finger, taking out most of the guesswork and experiments from the design. It defines a very stringent set of rules that if the finger complies with, it will be successful. Future work could then focus in supplementing the existing theoretical models that define criteria in which fingers with negative contact forces are not discarded.

The use of ANOVA has been illustrated and it has been shown to be potentially useful in the determination of the viability of the design. Even though the analysis showed that many interactions are statistically significant, it was to be expected

given the sensitivity of the fitness function. As the number of phalanges increases, the fully positive force workspace of an underactuated finger is drastically reduced, and the requirement of having a positive contact force on each phalanx becomes burdensome. New research could focus in theoretical alternatives where not all contact forces have to be positive, perhaps by studying the magnitude of the contact forces on a case by case basis, and also by taking explicit advantage of numerical simulations.

In conclusion, this thesis has presented the development of a new underactuated compliant gripper from the design of the joints that will eventually connect the various comprised links to the numerical simulations of the resulting design. The optimization at each stage was presented and the criteria used discussed.

REFERENCES

Bekey, G. A., Tomovic, R., and Zeljkovic, I. (1999). *Control Architecture of the Belgrade/USC Hand in Dextrous Robot Hands.* Springer-Verlag, New York, USA.

Berkelman, P., Cinquin, P., Boidard, E., Troccaz, J., Létoublon, C., and Ayoubi, J.-M. (2003). Design, control and testing of a novel compact laparoscopic endoscope manipulator. In *Proceedings of the Institution of Mechanical Engineers. Part 1: J. Systems and Control Engineering,* volume 217-4.

Birglen, L. (2004). *Analysis and Control of Underactuated Robotic Hands.* PhD thesis, Faculté des sciences et de génie, Université Laval, Québec, Canada.

Birglen, L. (2006). An introduction to the analysis of linkage-driven compliant underactuated fingers. In *2006 ASME International Design Engineering Technical Conferences,* Philadephia, PA, USA.

Birglen, L. and Gosselin, C. (2003). On the force capabilities of underactuated fingers. In *Proceedings of the 2003 IEEE International Conference on Robotics and Automation,* Taipei, Taiwan, pages 1139–1145.

Birglen, L. and Gosselin, C. (2004a). Kinetostatic analysis of underactuated fingers. *IEEE Transactions on Robotics and Automation,* **20**(2), 211–221.

Birglen, L. and Gosselin, C. (2004b). Optimal design of 2-phalanx underactuated fingers. In *Proceedings of 2004 International Conference on Intelligent Manipulation and Grasping,* Genova, Italy, pages 110–116.

Birglen, L. and Gosselin, C. (2005). Fuzzy enhanced control of an underactuated finger using tactile and position sensors. In *Proceedings of the 2005 IEEE International Conference on Robotics and Automation,* Barcelona, Spain, pages 2331–2336.

Birglen, L. and Gosselin, C. (2006a). Force analysis of connected differential mechanisms: Applications to grasping. *International Journal of Robotics Research*, **25**(10), 1033–1046.

Birglen, L. and Gosselin, C. (2006b). Geometric design of three-phalanx underactuated finger. *ASME Journal of Mechanical Design*, **128**(2), 356–364.

Birglen, L. and Gosselin, C. (2006c). Grasp-state plane analysis of two-phalanx underactuated fingers. *Mechanism and Machine Theory*, **41**(7), 807–822.

Birglen, L. and Gosselin, C. (2006d). Optimally unstable underactuated gripper: Synthesis and applications. In *2006 ASME International Design Engineering Technical Conferences*, Philadephia, PA, USA.

Birglen, L., Gosselin, C., Pouliot, N., Monsarrat, B., and Laliberté, T. (2002). Shade, a new 3-dof haptic device. *IEEE Transactions on Robotics and Automation*, **18**(2), 166–175.

Birglen, L., Laliberté, T., and Gosselin, C. (2008). *Underactuated Robotic Hands*. Springer. ISBN: 978-3-540-77458-7.

Boudreault, E. (2006). Conception de Préhenseurs Sous-Actionnés avec Articulations Déformables. Master's thesis, Université Laval, Québec, Canada.

Boudreault, E. and Gosselin, C. (2005). Mechanically intelligent grippers for telemedicine. In *Poster presented at the 15th Annual Canadian Conference on Intelligent Systems*, Québec, Canada.

Boudreault, E. and Gosselin, C. (2006). Design of sub-centimetre underactuated compliant grippers. In *Proceedings of 2006 ASME International Design Engineering Technical Conferences and Computers and Information In Engineering Conference, DETC2006*, volume v 2006, Philadephia, PA, USA.

Carrozza, M., Suppo, C., Sebastiani, F., Massa, B., Vecchi, F., Lazzarini, R., Cutkosky, M. R., and Dario, P. (2004). The spring hand: Development of a self-adaptive prosthesis for restoring natural grasping. *Autonomous Robots*, **16**(2), 125–141. Available from: http://dx.doi.org/10.1023/B:AURO.0000016863.48502.98.

Carrozza, M. C., Cappiello, G., Stellin, G., Zaccone, F., Vecchi, F., Mincera, S., and Dario, P. (2005). A cosmetic prosthetic hand with tendon driven under-actuated mechanism and compliant joints: Ongoing research and preliminary results. In *Proceedings of the 2005 IEEE International Conference on Robotics and Automation*, Barcelona, Spain, pages 2661–2666.

Carrozza, M. C., Massa, B., Micera, S., Lazzarini, R., Zecca, M., and Dario, P. (2002). The development of a novel prosthetic hand – ongoing research and preliminary results. *IEEE/ASME Transactions on Mechatronics*, **7**(2), 108–114.

Crowder, R. M. (1991). An anthropomorphic robotic end effector. *Robotics and Autonomous Systems*, **7**(4), 253–268.

de Bona, F. and Munteanu, M. G. (2005). Optimized flexural hinges for compliant micromechanisms. *Analog Integrated Circuits and Signal Processing*, **44**, 163–194.

de Visser, H. and Herder, J. L. (2000). Force directed design of a voluntary closing hand prosthesis. *Journal of Rehabilatation Research Dev*, **37**(3), 261–271.

Dean, A. M. and Voss, D. (1999). *Design and Analysis of Experiments*. Springer. ISBN: 978-0387985619.

Dechev, N., Cleghorn, W. L., and Naumann, S. (2001). Multiple finger, passive adaptive grasp prosthetic hand. *Mechanism and Machine Theory*, **36**, 1157–1173.

DeJong, K. and Spears, W. (1990). An analysis of the interacting roles of population size and crossover in genetic algorithms. In *Proceedings of the First Workshop in Parallel Problem Solving From Nature*, pages 38–47. Springer-Verlag.

Dilibal, S., Guner, E., and Akturk, N. (2002). Three-finger SMA robot hand and its practical analysis. *Robotica*, **20**(2), 175–180.

Dollar, A. and Howe, R. D. (2006). Joint coupling design of underactuated grippers. In *Proceedings of 2006 ASME International Design Engineering Technical Conferences and Computers and Information In Engineering Conference, DETC2006*, Philadephia, PA, USA.

Doshi, R., Yeh, C., and Leblanc, M. (1998). The design and development of a gloveless endoskeletal prosthetic hand. *Journal of Rehabilitation Research and Development*, **35**(4).

Dubey, V. and Crowder, R. M. (2002). A finger mechanism for adaptive end effectors. In *Proceedings of 2002 ASME Design Engineering Technical Conferences*, Montréal, Canada.

Eiselstein, L. (2005). Review of fatigue and fracture behavior in NiTi. In *Medical Device Materials III - Proceedings of the Materials and Processes for Medical Devices Conference*, Boston, MA, USA, pages 135–147.

Figliolini, G., Principe, M., and Rea, P. (2003). Mechatronic design of CA.U.M.HA. In *Proceedings of RAAD'03, 12 th International Workshop on Robotics in Alpe-Adria-Danube Region*, Cassino, Italy.

Fukaya, N., Toyama, S., Asfour, T., and Dillmann, R. (2000). Design of the tuat/karlsruhe humanoid hand. In *Proceedings of the 2000 IEEE/RSJ International Conference on Advanced Robotics*, Takamatsu, Japan, pages 1754–1759.

Gosselin, C. (2006). Adaptive robotic mechanical systems: A design paradigm. *ASME Journal of Mechanical Design*, **128**(1), 192–198.

Gosselin, C. and Laliberté, T. (1996). *Underactuated mechanical finger with return actuation*. U.S. Patent Office. US Patent No. 5 762 390.

Greiner, H. (1990). Passive and active grasping with a prehensile robot end-effector. Master's thesis, Massachusetts Institute of Technology, Artificial Intelligence Laboratory, Boston, MA, USA.

Henning, F. (1919). *Artificial Hand*. U.S. Patent Office. US Patent No. 1 298 502.

Herder, J. (2001). *Energy-free Systems; Theory, Conception and Design of Statically Balanced Spring Mechanisms*. PhD thesis, Delft University of Technology, Delft, The Netherlands.

Herder, J. L. and de Visser, H. (2000). Force directed design of a voluntary closing hand prosthesis. In *Proceedings of 2000 ASME Design Engineering Technical Conferences*, Baltimore, MD, USA, pages 1–8.

Hirose, S. (1985). Connected differential mechanisms and its applications. In *Proceedings of 1985 International Conference on Advanced Robotics*, Tokio, Japan, pages 319–325.

Hirose, S. and Umetani, Y. (1978). The development of soft gripper for the versatile robotic hand. *Mechanism and Machine Theory*, **13**, 351–358.

Houston, K., Sieber, A., Eder, C., Tonet, O., Menciassi, A., and Dario, P. (2007). Novel haptic tool and input device for real time bilateral biomanipulation addressing endoscopic surgery. In *Proceedings of the 2007 Annual International Conference of the IEEE EMBS*, Lyon, France.

Intuitive Surgical. EndoWrist Instrument and Accessory Catalog [online]. (2008). Available from: `http://www.intuitivesurgical.com/products/endowrist_instruments/index.aspx` [cited April 28, 2008].

Intuitive Surgical. Intuitive Surgical - EndoWrist Instruments [online]. (2008). Available from: `http://www.intuitivesurgical.com/products/endowrist_instruments/index.aspx` [cited April 28, 2008].

Itoh, H. (1975). *Mechanical Hand*. U.S. Patent Office. US Patent No. 3 927 424.

Johnson Matthey Metals. Johnson Matthey Metals [online]. (2008). Available from: `http://www.jmmedical.com` [cited April 28, 2008].

Kaneko, M. and Hayashi, T. (2003). Standing-up characteristic of contact force during self-posture changing motions. In *Proceedings of the 2003 IEEE International Conference on Robotics and Automation*, pages 202–208.

Kobayashi, E., Masamune, K., Sakuma, K., Dohi, T., and Hashimoto, D. (1999). A new safe laparoscopic manipulator system with a five-bar linkage mechanism and optical zoom. *Computer Aided Surgery*, 4(4), 182–192.

Kota, S., Lu, K.-J., Kreiner, Z., Trease, B., Arenas, J., and J.Geiger (2005). Design and application of compliant mechanisms for compliant tools. *Journal of Biomechanical Engineering*, **127**, 981–989.

Kyberd, P., Light, C., Chappel, P., Nightingale, J., Whatley, D., and Evans, M. (2001). The design of an antropomorphic prosthetic hand: A study of the southampton hand. *Robotica*, **19**(6), 593–600.

Laliberté, T., Birglen, L., and Gosselin, C. (2002). Underactuation in robotic grasping hands. *Japanese Journal of Machine Intelligence and Robotic Control, Special Issue on Underactuated Robots*, 4(3), 77–87.

Laliberté, T. and Gosselin, C. (1998). Simulation and design of underactuated mechanical hands. *Mechanism and Machine Theory*, **33**(1/2), 39–57.

Laliberté, T. and Gosselin, C. (2001). Underactuation in space robotic hands. In *International Symposium on Artificial Intelligence, Robotics and Automation in Space*, Montréal, Canada.

Laliberté, T. and Gosselin, C. (2003). *Actuation System for Highly Underactuated Gripping Mechanisms*. U.S. Patent Office. US Patent No. 6 505 870.

Lobontiu, N. (2002). *Compliant Mechanisms: Design of Flexure Hinges*. CRC. ISBN: 978-0849313677.

Lotti, F., Tiezzi, P., Vassura, G., Biagotti, L., Palli, G., and Melchiorri, C. (2005). Development of ub hand 3: Early results. In *Proceedings of the 2005 IEEE International Conference on Robotics and Automation*, Barcelona, Spain. IEEE.

Lotti, F. and Vassura, G. (2002). A novel approach to mechanical design of articulated fingers for robotic hands. In *Proceedings of the 2002 IEEE/RSJ International Conference on Intelligent Robots and Systems*, volume 2, pages 1687–1692.

Luo, M., Mei, T., Wang, X., and Yu, Y. (2004). Grasp characteristics of an underactuated robot hand. In *Proceedings of the 2004 IEEE International Conference on Robotics and Automation*, New Orleans, LA, USA, pages 2236–2241. IEEE.

Massa, B. and Gosselin, C. (2003). Design and development of an underactuated finger based on compliant mechanisms. In *2003 CCToMM Symposium on Mechanisms, Machines, and Mechatronics 2003 CCToMM Symposium on Mechanisms, Machines, and Mechatronics 2003 CCoTM Symposium on Mechanisms, Machines, and Mechatronics*, Montréal, Canada.

MatWeb. MatWeb: Material Property Data [online]. (2008). Available from: `http://www.matweb.com/` [cited April 28, 2008].

Montgomery, D. C. (2005). *Design and Analysis of Experiments*. Wiley. ISBN: 978-0-471-48735-7.

Mullen, J. (1972). *Mechanical Hand*. U.S. Patent Office. US Patent No. 3 694 021.

Nasser, S., Rincón, D., and Rodríguez, M. (2006). Design of an anthropomorphic underactuated hand prosthesis with passive-adaptive grasping capabilities. In *Proceedings of the 2006 Florida Conference on Recent Advances in Robotics and Robot Showcase*, Miami, FL, USA.

Norton, R. L. (2003). *Design of Machinery: An Introduction to the Synthesis and Analysis of Mechanisms and Machines*. McGraw-Hill Professional.

Petersen, R. G. (1985). *Design and Analysis of Experiments*. Marcel Dekker, Inc.

Rakic, M. (1989). Multifingered robot hand with selfadaptability. *Robotics and Computer-Integrated Manufacturing*, **3**(2/3), 269–276.

Robinson, G. and Davies, J. (1997). The amadeus project: An overview. *Industrial Robot*, **24**(4), 290–296.

Rout, B. and Mittal, R. (2006). Parametric design optimization of 2-dof r-r planar manipulator-a design of experiment approach. *Robotics and Computer-Integrated Manufacturing*, **24**, 239–248.

Rovetta, A. (1981). On functionality of a new mechanical hand. *ASME Journal of Mechanical Design*, **103**, 277–280.

Rovetta, A., Franchetti, I., and Vicentini, P. (1982). *Multi-Purpose Mechanical Hand*. U.S. Patent Office. US Patent No. 4 351 553.

Rudolph, G. (1994). Convergence analysis of canonical genetic algorithms. *IEEE Transactions on Neural Networks*, **5**(1).

Schmidt, H. and Ulrich, M. L. (2004). *Surgical anatomy of the Hand*. Thieme Medical Publishers.

Schulz, S., Pylatiuk, C., and Bretthauer, G. (2001). A new ultralight anthropomorphic hand. In *Proceedings of the 2001 IEEE International Conference on Robotics and Automation*, Seoul, Korea, pages 2437–2441.

Shimojima, H., Yamamoto, K., and Kawakita, K. (1987). A study of grippers with multiple degrees of mobility. *JSME International Journal*, **30**(261), 515–522.

Shiu, Y. Y. and Cheung, B. (2006). Bounds for probability of success of classical genetic algorithm based on hamming distance. *IEEE Transactions on Evolutionary Computation*, **10**(1), 1–18.

Sun, L.-W., Meer, F. V., Bailly, Y., and Yeung, C. K. (2007). Design and development of a da vinci surgical system simulator. In *Proceedings of the 2007 IEEE International Conference on Mechatronics and Automation*, Harbin, China.

Ullmann, E., Cepolina, F., and Zoppi, M. (2004). Upper limb prosthetics for developing countries. In *Proceedings of 2004 International Conference on Intelligent Manipulation and Grasping*, Genova, Italy, pages 225–226.

Wikimedia. Wikimedia commons [online]. (2008). Available from: `http://commons.wikimedia.org/wiki/Main_Page` [cited April 28, 2008].

Wilkes, K. and Liaw, P. (2000). The fatigue behavior of shape-memory alloys. *JOM Journal of the Minerals, Metals and Materials Society*, **52**(10), 45–51. Available from: `http://dx.doi.org/10.1007/s11837-000-0083-3`.

Yang, J., Adbel-Malek, K., and Pitarch, E. P. (2004). Design and analysis of a cable actuated hand prosthesis. In *Proceedings of 2004 ASME Design Engineering Technical Conference and Computers in Engineering Conference*, Salt Lake City, UT, USA.

Yoshida, K. and Nakanishi, H. (2001). The TAKO (target collaborative) flyer: a new concept for future satellite servicing. In *Proceedings of the 6th International Symposium on Artificial Intelligence and Robotics & Automation in Space: i-SAIRAS*, Saint-Hubert, QC, Canada.

Zecca, M., Cappiello, G., Sebastiani, F., Roccella, S., Vecchi, F., Carrozza, M. C., and Dario, P. (2003). Experimental analysis of the proprioceptive and exteroceptive sensors of an underactuated prosthetic hand. *International Journal of Human-friendly Welfare Robotic Systems*, 4(4), 2–6.

APPENDIX I

ANOVA RESULTS

Below are the results of the ANOVA with a p-value equal or less than 0.05 which are considered statistically significant.

Source	F	Prob>F	Source	F	Prob>F
A2	7.126	0.022	A2*B3*C3	28.185	0.000
A3	6.982	0.023	A2*C3*Psi	32.044	0.000
B3	5.210	0.043	B2*C2*C3	8.114	0.016
C3	31.491	0.000	B2*A3*C3	15.896	0.002
A1*A2	14.900	0.003	B2*B3*C3	14.651	0.003
B1*C3	6.436	0.028	B2*C3*Psi	6.794	0.024
C1*C3	12.703	0.004	C2*A3*C3	16.317	0.002
A2*B2	6.033	0.032	C2*B3*C3	13.656	0.004
A2*A3	8.515	0.014	C2*C3*Psi	10.716	0.007
A2*C3	43.398	0.000	A3*B3*C3	34.265	0.000
A2*Psi	5.564	0.038	A3*B3*Psi	5.248	0.043
B2*C3	15.850	0.002	A3*C3*Psi	16.303	0.002
C2*C3	17.250	0.002	B3*C3*Psi	16.662	0.002
A3*B3	7.379	0.020	A1*B1*C1*C3	7.596	0.019
A3*C3	29.108	0.000	A1*B1*A2*B3	6.747	0.025
B3*C3	26.741	0.000	A1*B1*A2*C3	9.386	0.011
C3*Psi	18.112	0.001	A1*B1*B2*C3	7.170	0.021
A1*B1*C3	10.761	0.007	A1*B1*C2*C3	5.407	0.040
A1*C1*A2	6.718	0.025	A1*B1*A3*C3	8.112	0.016
A1*C1*C3	5.601	0.037	A1*B1*C3*Psi	5.359	0.041
A1*A2*B2	4.849	0.050	A1*C1*A2*C2	6.266	0.029
A1*A2*C2	13.414	0.004	A1*C1*A2*A3	6.516	0.027
A1*A2*A3	13.278	0.004	A1*C1*A2*B3	30.551	0.000
A1*A2*B3	59.375	0.000	A1*C1*B2*C3	6.583	0.026
A1*A2*C3	6.453	0.027	A1*C1*C3*Psi	5.409	0.040
A1*A2*Psi	7.934	0.017	A1*A2*B2*C2	5.439	0.040
A1*B2*C3	8.211	0.015	A1*A2*B2*B3	27.485	0.000
A1*C2*B3	4.916	0.049	A1*A2*C2*A3	11.892	0.005
B1*A2*C3	22.579	0.001	A1*A2*C2*B3	52.855	0.000
C1*A2*C3	25.943	0.000	A1*A2*C2*C3	5.853	0.034
C1*B2*C3	5.091	0.045	A1*A2*C2*Psi	5.496	0.039
C1*C2*C3	6.420	0.028	A1*A2*A3*B3	51.023	0.000
C1*A3*C3	10.985	0.007	A1*A2*A3*C3	9.252	0.011
C1*B3*C3	11.236	0.006	A1*A2*A3*Psi	7.062	0.022
C1*C3*Psi	6.475	0.027	A1*A2*B3*C3	41.661	0.000
A2*B2*A3	7.582	0.019	A1*A2*B3*Psi	36.675	0.000
A2*B2*C3	34.462	0.000	A1*B2*C2*C3	5.125	0.045
A2*C2*C3	30.580	0.000	A1*B2*A3*C3	8.765	0.013
A2*A3*B3	5.457	0.039	A1*B2*C3*Psi	5.924	0.033
A2*A3*C3	44.374	0.000	B1*C1*A2*C3	11.074	0.007
A2*A3*Psi	6.852	0.024	B1*A2*B2*C3	10.401	0.008
continued...			*continued...*		

Source	F	Prob>F		Source	F	Prob>F
B1*A2*C2*C3	12.648	0.005		A1*C1*B2*C3*Psi	5.119	0.045
B1*A2*A3*C3	19.188	0.001		A1*C1*C2*C3*Psi	5.601	0.037
B1*A2*B3*C3	15.504	0.002		A1*A2*B2*C2*B3	27.602	0.000
B1*A2*C3*Psi	11.369	0.006		A1*A2*B2*A3*B3	20.529	0.001
C1*A2*B2*C3	14.690	0.003		A1*A2*B2*B3*C3	12.320	0.005
C1*A2*C2*C3	16.625	0.002		A1*A2*B2*B3*Psi	15.682	0.002
C1*A2*A3*C3	24.874	0.000		A1*A2*C2*A3*B3	46.113	0.000
C1*A2*B3*C3	20.473	0.001		A1*A2*C2*A3*C3	8.831	0.013
C1*A2*C3*Psi	17.723	0.001		A1*A2*C2*B3*C3	39.072	0.000
C1*B2*B3*C3	4.997	0.047		A1*A2*C2*B3*Psi	29.693	0.000
C1*C2*A3*C3	5.696	0.036		A1*A2*A3*B3*C3	45.843	0.000
C1*C2*B3*C3	5.123	0.045		A1*A2*A3*B3*Psi	31.615	0.000
C1*A3*B3*C3	14.078	0.003		A1*A2*A3*C3*Psi	6.754	0.025
C1*A3*C3*Psi	5.408	0.040		A1*A2*B3*C3*Psi	28.997	0.000
C1*B3*C3*Psi	6.384	0.028		A1*B2*C2*A3*C3	5.674	0.036
A2*B2*C2*C3	22.345	0.001		A1*B2*C2*C3*Psi	5.657	0.037
A2*B2*A3*B3	7.585	0.019		A1*B2*A3*B3*C3	5.895	0.034
A2*B2*A3*C3	37.642	0.000		A1*B2*A3*C3*Psi	6.192	0.030
A2*B2*A3*Psi	5.577	0.038		B1*C1*A2*C2*C3	5.822	0.034
A2*B2*B3*C3	28.601	0.000		B1*C1*A2*A3*C3	7.734	0.018
A2*B2*C3*Psi	22.001	0.001		B1*C1*A2*B3*C3	8.510	0.014
A2*C2*A3*C3	32.766	0.000		B1*C1*A2*C3*Psi	4.914	0.049
A2*C2*A3*Psi	5.048	0.046		B1*A2*B2*A3*C3	8.899	0.012
A2*C2*B3*C3	20.437	0.001		B1*A2*B2*B3*C3	8.087	0.016
A2*C2*C3*Psi	25.929	0.000		B1*A2*C2*A3*C3	10.800	0.007
A2*A3*B3*C3	44.683	0.000		B1*A2*C2*B3*C3	8.020	0.016
A2*A3*B3*Psi	6.235	0.030		B1*A2*C2*C3*Psi	6.589	0.026
A2*A3*C3*Psi	33.009	0.000		B1*A2*A3*B3*C3	22.831	0.001
A2*B3*C3*Psi	24.561	0.000		B1*A2*A3*C3*Psi	9.399	0.011
B2*C2*A3*C3	8.715	0.013		B1*A2*B3*C3*Psi	7.160	0.022
B2*C2*B3*C3	6.830	0.024		C1*A2*B2*C2*C3	9.266	0.011
B2*A3*B3*C3	20.990	0.001		C1*A2*B2*A3*C3	15.464	0.002
B2*A3*C3*Psi	6.922	0.023		C1*A2*B2*B3*C3	14.247	0.003
B2*B3*C3*Psi	7.085	0.022		C1*A2*B2*C3*Psi	7.898	0.017
C2*A3*B3*C3	19.140	0.001		C1*A2*C2*A3*C3	17.170	0.002
C2*A3*C3*Psi	9.983	0.009		C1*A2*C2*B3*C3	13.294	0.004
C2*B3*C3*Psi	9.376	0.011		C1*A2*C2*C3*Psi	13.862	0.003
A3*B3*C3*Psi	21.565	0.001		C1*A2*A3*B3*C3	30.663	0.000
A1*B1*C1*A2*C3	7.719	0.018		C1*A2*A3*C3*Psi	17.655	0.001
A1*B1*A2*B2*C3	8.435	0.014		C1*A2*B3*C3*Psi	16.659	0.002
A1*B1*A2*C2*B3	9.521	0.010		C1*B2*A3*B3*C3	7.341	0.020
A1*B1*A2*C2*C3	4.902	0.049		C1*C2*A3*B3*C3	7.240	0.021
A1*B1*A2*A3*C3	6.032	0.032		C1*A3*B3*C3*Psi	8.283	0.015
A1*B1*A2*B3*Psi	6.008	0.032		A2*B2*C2*A3*C3	26.868	0.000
A1*B1*A2*C3*Psi	5.020	0.047		A2*B2*C2*B3*C3	18.991	0.001
A1*B1*B2*A3*C3	5.651	0.037		A2*B2*C2*C3*Psi	17.137	0.002
A1*B1*A3*B3*C3	5.699	0.036		A2*B2*A3*B3*C3	47.835	0.000
A1*C1*A2*B2*B3	14.932	0.003		A2*B2*A3*B3*Psi	7.495	0.019
A1*C1*A2*C2*A3	6.105	0.031		A2*B2*A3*C3*Psi	25.652	0.000
A1*C1*A2*C2*B3	28.123	0.000		A2*B2*B3*C3*Psi	21.672	0.001
A1*C1*A2*A3*B3	27.936	0.000		A2*C2*A3*B3*C3	36.342	0.000
A1*C1*A2*B3*C3	19.491	0.001		A2*C2*A3*B3*Psi	5.332	0.041
A1*C1*A2*B3*Psi	16.109	0.002		A2*C2*A3*C3*Psi	28.634	0.000
A1*C1*B2*A3*C3	6.365	0.028		A2*C2*B3*C3*Psi	21.384	0.001
continued...				*continued...*		

Source	F	Prob>F
A2*A3*B3*C3*Psi	39.885	0.000
B2*C2*A3*B3*C3	11.597	0.006
B2*A3*B3*C3*Psi	10.967	0.007
C2*A3*B3*C3*Psi	13.455	0.004
A1*B1*C1*A2*C2*C3	4.879	0.049
A1*B1*A2*B2*C2*B3	6.495	0.027
A1*B1*A2*B2*A3*C3	6.267	0.029
A1*B1*A2*C2*A3*B3	7.398	0.020
A1*B1*A2*C2*B3*Psi	7.509	0.019
A1*B1*B2*A3*B3*C3	6.116	0.031
A1*C1*A2*B2*C2*B3	15.317	0.002
A1*C1*A2*B2*A3*B3	11.793	0.006
A1*C1*A2*B2*B3*C3	6.275	0.029
A1*C1*A2*B2*B3*Psi	6.308	0.029
A1*C1*A2*C2*A3*B3	27.030	0.000
A1*C1*A2*C2*B3*C3	19.772	0.001
A1*C1*A2*C2*B3*Psi	12.014	0.005
A1*C1*A2*A3*B3*C3	25.194	0.000
A1*C1*A2*A3*B3*Psi	14.501	0.003
A1*C1*A2*B3*C3*Psi	11.764	0.006
A1*C1*B2*C2*C3*Psi	6.201	0.030
A1*C1*B2*A3*B3*C3	6.114	0.031
A1*C1*B2*A3*C3*Psi	5.198	0.044
A1*A2*B2*C2*A3*B3	21.379	0.001
A1*A2*B2*C2*B3*C3	14.205	0.003
A1*A2*B2*C2*B3*Psi	13.004	0.004
A1*A2*B2*A3*B3*C3	10.472	0.008
A1*A2*B2*A3*B3*Psi	10.827	0.007
A1*A2*B2*B3*C3*Psi	8.410	0.014
A1*A2*C2*A3*B3*C3	45.825	0.000
A1*A2*C2*A3*B3*Psi	25.095	0.000
A1*A2*C2*B3*C3*Psi	23.368	0.001
A1*A2*A3*B3*C3*Psi	35.966	0.000
A1*B2*C2*A3*C3*Psi	6.645	0.026
A1*B2*A3*B3*C3*Psi	6.026	0.032
B1*C1*A2*A3*B3*C3	11.610	0.006
B1*A2*B2*A3*B3*C3	14.065	0.003
B1*A2*C2*A3*B3*C3	14.067	0.003
B1*A2*C2*A3*C3*Psi	5.393	0.040
B1*A2*A3*B3*C3*Psi	12.682	0.004
C1*A2*B2*C2*A3*C3	11.427	0.006
C1*A2*B2*C2*B3*C3	9.512	0.010
C1*A2*B2*C2*C3*Psi	6.874	0.024
C1*A2*B2*A3*B3*C3	24.998	0.000
C1*A2*B2*A3*C3*Psi	9.621	0.010
C1*A2*B2*B3*C3*Psi	10.079	0.009
C1*A2*C2*A3*B3*C3	23.728	0.000
C1*A2*C2*A3*C3*Psi	15.728	0.002
C1*A2*C2*B3*C3*Psi	14.250	0.003
C1*A2*A3*B3*C3*Psi	27.415	0.000
C1*C2*A3*B3*C3*Psi	5.249	0.043
A2*B2*C2*A3*B3*C3	38.614	0.000
A2*B2*C2*A3*B3*Psi	6.637	0.026
A2*B2*C2*A3*C3*Psi	23.081	0.001
A2*B2*C2*B3*C3*Psi	18.527	0.001
A2*B2*A3*B3*C3*Psi	40.508	0.000
A2*C2*A3*B3*C3*Psi	39.614	0.000
B2*C2*A3*B3*C3*Psi	7.180	0.021
A1*B1*A2*B2*C2*B3*Psi	5.884	0.034
A1*B1*A2*C2*A3*B3*Psi	6.174	0.030
A1*C1*A2*B2*C2*A3*B3	13.074	0.004
A1*C1*A2*B2*C2*B3*C3	7.921	0.017
A1*C1*A2*B2*A3*B3*C3	6.751	0.025
A1*C1*A2*C2*A3*B3*C3	29.678	0.000
A1*C1*A2*C2*A3*B3*Psi	10.348	0.008
A1*C1*A2*C2*B3*C3*Psi	8.547	0.014
A1*C1*A2*A3*B3*C3*Psi	18.567	0.001
A1*C1*B2*C2*A3*B3*C3	5.133	0.045
A1*C1*B2*C2*A3*B3*Psi	5.028	0.047
A1*C1*B2*C2*A3*C3*Psi	7.937	0.017
A1*C1*B2*C2*B3*C3*Psi	6.188	0.030
A1*C1*B2*A3*B3*C3*Psi	8.724	0.013
A1*A2*B2*C2*A3*B3*C3	13.492	0.004
A1*A2*B2*C2*A3*B3*Psi	7.893	0.017
A1*A2*B2*C2*B3*C3*Psi	6.515	0.027
A1*A2*B2*A3*B3*C3*Psi	7.977	0.017
A1*A2*C2*A3*B3*C3*Psi	31.872	0.000
A1*B2*C2*A3*B3*C3*Psi	8.276	0.015
B1*C1*A2*C2*A3*B3*C3	7.049	0.022
B1*C1*A2*A3*B3*C3*Psi	6.176	0.030
B1*A2*B2*C2*A3*B3*C3	8.140	0.016
B1*A2*B2*A3*B3*C3*Psi	5.509	0.039
B1*A2*C2*A3*B3*C3*Psi	8.326	0.015
C1*A2*B2*C2*A3*B3*C3	22.784	0.001
C1*A2*B2*C2*A3*B3*Psi	5.862	0.034
C1*A2*B2*C2*A3*C3*Psi	11.193	0.007
C1*A2*B2*C2*B3*C3*Psi	10.628	0.008
C1*A2*B2*A3*B3*C3*Psi	22.895	0.001
C1*A2*C2*A3*B3*C3*Psi	29.811	0.000
A2*B2*C2*A3*B3*C3*Psi	44.777	0.000
A1*B1*A2*B2*C2*A3*B3*Psi	4.851	0.050
A1*C1*A2*B2*C2*A3*B3*C3	11.574	0.006
A1*C1*A2*C2*A3*B3*C3*Psi	17.967	0.001
A1*C1*B2*C2*A3*B3*C3*Psi	20.991	0.001
A1*A2*B2*C2*A3*B3*C3*Psi	5.863	0.034
B1*C1*B2*C2*A3*B3*C3*Psi	6.497	0.027
C1*A2*B2*C2*A3*B3*C3*Psi	40.784	0.000

continued...